Primate phylogenomics uncovers multiple rapid radiations and ancient interspecific introgression

Dan Vanderpool[1]*, Bui Quang Minh[2,3], Robert Lanfear[3], Daniel Hughes[4], Shwetha Murali[4], R. Alan Harris[4,5], Muthuswamy Raveendran[4], Donna M. Muzny[4,5], Richard A. Gibbs[4,5], Kim C. Worley[4,5], Jeffrey Rogers[4,5], Matthew W. Hahn[1]

[1]Department of Biology and Department of Computer Science, Indiana University, 1001 E. 3rd Street, Bloomington, IN 47405, USA.

[2]Research School of Computer Science, Australian National University, 145 Science Road, Canberra, ACT 2601, Australia.

[3]Research School of Biology, Australian National University, 46 Sullivans Creek Road, Canberra, ACT 2601, Australia.

[4]Human Genome Sequencing Center, Baylor College of Medicine, One Baylor Plaza, Houston, TX 77030, USA.

[5]Department of Molecular and Human Genetics, Baylor College of Medicine, One Baylor Plaza, Houston, TX 77030, USA.

*danvand@indiana.edu

Abstract

Our understanding of the evolutionary history of primates is undergoing continual revision due to ongoing genome sequencing efforts. Bolstered by growing fossil evidence, these data have led to increased acceptance of once controversial hypotheses regarding phylogenetic relationships, hybridization and introgression, and the biogeographical history of primate groups. Among these findings is a pattern of recent introgression between species within all major primate groups examined to date, though little is known about introgression deeper in time. To address this and other phylogenetic questions, here we present new reference genome assemblies for three Old World Monkey species: *Colobus angolensis ssp. palliatus* (the black and white colobus), *Macaca nemestrina* (southern pig-tailed macaque), and *Mandrillus leucophaeus* (the drill). We combine these data with 23 additional primate genomes to estimate both the species tree and individual gene trees using thousands of loci. While our species tree is largely consistent with previous phylogenetic hypotheses, the gene trees reveal high levels of genealogical discordance associated with multiple primate radiations. We use strongly asymmetric patterns of gene tree discordance around specific branches to identify multiple instances of introgression between ancestral primate lineages. In addition, we exploit recent fossil evidence to perform fossil-calibrated molecular dating analyses across the tree. Taken together, our genome-wide data help to resolve multiple contentious sets of relationships among primates, while also providing insight into the biological processes and technical artifacts that led to the disagreements in the first place.

Introduction

Understanding the history of individual genes and whole genomes is an important goal for evolutionary biology. It is only by understanding these histories that we can understand the origin and evolution of traits—whether morphological, behavioral, or biochemical. Until recently, our ability to address the history of genes and genomes was limited by the availability of comparative genomic data. However, genome sequences are now being generated extremely rapidly. In primates alone, there are already 23 species with published reference genome sequences and associated annotations (Table S1), as well as multiple species with population samples of whole genomes [1–11]. These data can now be used to address important evolutionary questions.

Several studies employing dozens of loci sampled across broad taxonomic groups have provided rough outlines of the evolutionary relationships and divergence times among primates [12,13]. Due to the rapid nature of several independent radiations within primates, these limited data cannot resolve species relationships within some clades [12–14]. For instance, the New World Monkeys (NWM) experienced a rapid period of diversification ~15-18 million years ago (mya) [15] (Figure 1), resulting in ambiguous relationships among the three Cebidae subfamilies (Cebinae=squirrel monkeys and capuchins, Aotinae=owl monkeys, and Callitrichinae=marmosets and tamarins) [12–14,16–18]. High levels of incomplete lineage sorting (ILS) driven by short times between the divergence of distinct lineages have led to a large amount of gene tree discordance in the NWM, with different loci favoring differing relationships among

65 taxa. Given the known difficulties associated with resolving short internodes [19–21], as
66 well as the multiple different approaches and datasets used in these analyses, the
67 relationships among cebid subfamilies remain uncertain.

68 In addition to issues of limited data and rapid radiations, a history of hybridization
69 and subsequent gene flow between taxa means that there is no single dichotomously
70 branching tree that all genes follow. Although it once was thought to be relatively rare
71 (especially among animals, [22]), genomic studies have uncovered widespread patterns
72 of recent introgression across the tree of life [23]. Evidence for recent or ongoing gene
73 flow is especially common among the primates (e.g. [9,24–27]), sometimes with clear
74 evidence for adaptive introgression (e.g. [28–30]). Whether widespread gene flow
75 among primates is emblematic of their initial radiation (which began 60-75 mya, [13,31–
76 33]) or is a consequence of current conditions—which include higher environmental
77 occupancy and more secondary contact—remains an open question [34].

78 Here we report the sequencing and annotation of three new primate genomes, all
79 Old World Monkey (OWM) species: *Colobus angolensis ssp. palliatus* (the black and
80 white colobus), *Macaca nemestrina* (southern pig-tailed macaque), and *Mandrillus*
81 *leucophaeus* (the drill). Together with the published whole genomes of extant primates,
82 we present a phylogenomic analysis including 26 primate species and several closely
83 related non-primates. Incorporating recently discovered fossil evidence [35], we perform
84 fossil-calibrated molecular dating analyses to estimate divergence times, including
85 dates for the crown primates as well as the timing of more recent splits. Compared to
86 recent hybridization, introgression that occurred between two or more ancestral
87 lineages (represented by internal branches on a phylogeny) is difficult to detect. To get

around this limitation, we modify a previously proposed method for detecting introgression [36] and apply it to our whole-genome datasets, finding additional evidence for gene flow among ancestral primates. Finally, we closely examine the genealogical patterns left behind by the NWM radiation, as well as the biases of several methods that have been used to resolve this topology. We use multiple approaches to provide a strongly supported history of the NWM and primates in general, while also highlighting the large amounts of gene tree discordance across the tree caused by ILS and introgression.

Results and Discussion

Primate Genome Sequencing

The assembly and annotation of each of the three species sequenced for this project are summarized here, with further details listed in Table 1. A summary of all published genomes used in this study, including links to the assemblies and NCBI BioProjects, is available in Table S2.

The sequencing effort for *Colobus angolensis ssp. palliatus* produced 514 Gb of data, which are available in the NCBI Short Read Archive (SRA) under the accession SRP050426 (BioProject PRJNA251421). Assembly of these data resulted in a total assembly length of 2.97 Gb in 13,124 scaffolds (NCBI assembly Cang.pa_1.0; GenBank accession GCA_000951035.1) with an average per base coverage of 86.8X. Subsequent annotation via the NCBI Eukaryotic Genome Annotation Pipeline (annotation release ID: 100) resulted in the identification of 20,222 protein-coding genes

and 2,244 non-coding genes. An assessment of the annotation performed using BUSCO 3.0.2 [37] in conjunction with the Euarchontoglires ortholog database 9 (https://busco-archive.ezlab.org/v3/datasets/euarchontoglires_odb9.tar.gz) indicated that 95.82% complete or fragmented single-copy orthologs (91.68% complete, 4.13% fragmented) were present among the annotated protein-coding genes. Comprehensive annotation statistics for *C. angolensis ssp. palliatus* with links to the relevant annotation products available for download can be viewed at https://www.ncbi.nlm.nih.gov/genome/annotation_euk/Colobus_angolensis_palliatus/100/.

For *Macaca nemistrina*, 1,271 Gb of data were produced (SRA accession SRP045960; BioProject PRJNA2791) resulting in an assembled genome length of 2.95 Gb in 9,733 scaffolds (Mnem_1.0; GenBank accession GCF_000956065.1). This corresponds to an average per base coverage of 113.1X when both short and long-read data are combined (Materials and Methods). The NCBI annotation resulted in 21,017 protein coding genes and 13,163 non-coding genes (annotation release ID: 101). A BUSCO run to assess the completeness of the annotation (as above) indicated 95.98% complete or fragmented single-copy orthologs (92.23% complete, 3.75% fragmented) present among the annotated protein-coding genes. Comprehensive annotation statistics for *M. nemistrina* with links to the relevant annotation products available for download can be viewed at https://www.ncbi.nlm.nih.gov/genome/annotation_euk/Macaca_nemestrina/101/.

Sequencing of *Mandrillus leucophaeus* libraries resulted in 334.1 Gb of data (SRA accession SRP050495; BioProject PRJNA251423) that once assembled resulted

in a total assembly length of 3.06 Gb in 12,821 scaffolds (Mleu.le_1.0; GenBank accession GCA_000951045.1) with an average coverage of 117.2X per base. The NCBI annotation produced of 20,465 protein coding genes and 2,300 non-coding genes (annotation release ID: 100). A BUSCO run to assess the completeness of the annotation (as above) indicated 95.45% complete or fragmented single-copy orthologs (91.38% complete, 4.07% fragmented) present among the annotated protein-coding genes. The full annotation statistics with links to the associated data can be viewed at https://www.ncbi.nlm.nih.gov/genome/annotation_euk/Mandrillus_leucophaeus/100/.

Phylogenetic Relationships Among Primates

To investigate phylogenetic relationships among primates, we selected the longest isoform for each protein-coding gene from 26 primate species and 3 non-primate species (Table S1). After clustering, aligning, trimming, and filtering (Materials and Methods) there were 1,730 single-copy orthologs present in at least 27 of the 29 species. These cutoffs ensure high species coverage while still retaining a large number of orthologs. The coding sequences of these orthologs have an average length of 1,018 bp and 178 parsimony-informative characters per gene. Concatenation of these loci resulted in an alignment of 1,761,114 bp, with the fraction of gaps/ambiguities varying from 4.04% (*Macaca mulatta*) to 18.37% (*Carlito syrichta*) (Table S3). We then inferred the species tree using both gene tree (as implemented in ASTRAL III, [38] and concatenation (as implemented in IQ-TREE 2; [39]) approaches.

We inferred 1,730 individual gene trees from nucleotide alignments using maximum likelihood in IQ-TREE 2, and then used these gene tree topologies as input to

ASTRAL III (Materials and Methods). We used the mouse, *Mus musculus*, as an outgroup to root the species tree. This approach resulted in a topology (which we refer to as "ML-ASTRAL"; Figure 1) that largely agrees with previously published phylogenies [12,13]. Maximum likelihood analysis of the concatenated nucleotide alignment (which we refer to as "ML-CONCAT") using IQ-TREE resulted in a topology that differed from the ML-ASTRAL tree only with respect to the placement of *Aotus nancymaae* (owl monkey): rather than sister to the *Saimiri*+*Cebus* clade (as in Figure 1), the ML-CONCAT tree places *Aotus* sister to *Callithrix jacchus*, a minor rearrangement around a very short internal branch (Figure 1). All branches of the ML-ASTRAL species tree are supported by maximum local posteriors [40], except for the branch that defines *Aotus* as sister to the *Saimiri*+*Cebus* clade (0.46 local posterior probability). Likewise, each branch in the ML-CONCAT tree is supported by 100% bootstrap values, including the branch uniting *Aotus* and *Callithrix*. We return to this conflict in the next section.

There has been some contention as to the placement of the mammalian orders Scandentia (treeshrews) and Dermoptera (colugos) [41–50]. Both the ML-ASTRAL and ML-CONCAT trees place these two groups outside the Primates with maximal statistical support (i.e. local posterior probabilities of 1.0 and bootstrap values of 100%; Figure 1), with Dermoptera as the closest sister lineage to the Primates [12,51–53]. However, while support values such as the bootstrap or posterior provide statistical confidence in the species tree topology, there can be large amounts of underlying gene tree discordance even for branches with 100% support (e.g. [54–56]). To assess discordance generally, and the relationships among the Primates, Scandentia, and Dermoptera in particular, we used IQ-TREE to calculate both gene (gCF) and site (sCF)

177 concordance factors [57] for each internal branch of the topology in Figure 1. These two
178 measures represent the fraction of genes and sites, respectively, that are in agreement
179 with the species tree for any particular branch.

180 Examining concordance factors helps to explain previous uncertainty in the
181 relationships among Primates, Scandentia, and Dermoptera (Figure 1). Although the
182 bootstrap support is 100% and the posterior probability is 1.0 on the branch leading to
183 the Primate common ancestor, the gene concordance factor is 45% and the site
184 concordance factor is 39%. These values indicate that, of decisive gene trees (*n*=1663),
185 only 45% of them contain the branch that is in the species tree; this branch reflects the
186 Primates as a single clade that excludes Scandentia and Dermoptera. While the
187 species tree represents the single topology supported by the most gene trees (hence
188 the strong statistical support for this branch), the concordance factors also indicate that
189 a majority of individual topologies have histories that differ from the estimated species
190 tree. In fact, the gCF value indicates that 55% of trees do not support a monophyletic
191 Primate order, with either Dermoptera, Scandentia, or both lineages placed within
192 Primates. Likewise, the sCF value indicates that only 39% of parsimony-informative
193 sites in the total alignment support the branch uniting all primates, with 30% favoring
194 Dermoptera as sister to the Primate sub-order Strepsirrhini and 31% placing
195 Dermoptera sister to the Primate sub-order Haplorrhini. Similarly, only a small plurality
196 of genes and sites have histories that place Dermoptera as sister to the Primates rather
197 than either of the two alternative topologies (gCF=37, sCF=40; Figure 1), despite the
198 maximal statistical support for these relationships. While discordance at individual gene
199 trees can result from technical problems in tree inference (e.g. long-branch attraction,

low phylogenetic signal, poorly aligned sequences, or model misspecification), it also often reflects biological causes of discordance such as incomplete lineage sorting and introgression. The fraction of discordant gene trees for branches near the base of the primate tree is no larger than the fraction on branches reflecting more recent radiations (Figure 1), and therefore likely results from both technical errors and the biological consequences of the rapid radiation of mammalian lineages during this period [32,51,58,59].

Within the Primates, the phylogenetic affiliation of tarsiers (represented here by *Carlito syrichta*) has been debated since the first attempts by Buffon (1765) and Linnaeus (1767-1770) to systematically organize described species [60]. Two prevailing hypotheses group tarsiers (Tarsiiformes) with either lemurs and lorises (the “prosimian” hypothesis, [61]) or with Simiiformes (the “Haplorrhini” hypothesis, [62], where Simiiformes = Apes+OWM+NWM). The ML-ASTRAL and ML-CONCAT analyses place Tarsiiformes with Simiiformes, supporting the Haplorrhini hypothesis (Figure 1). The strepsirrhines come out as a well-supported group sister to the other primates. Again, our inference of species relationships is consistent with previous genomic analyses [58,63], but also highlights the high degree of discordance in this part of the tree. The rapid radiation of mammalian lineages that occurred in the late Paleocene and early Eocene [32] encompassed many of the basal primate branches, including the lineage leading to Haplorrhini. The complexity of this radiation is likely the reason for low gCF and sCFs (39.5% and 36%, respectively) for the branch leading to Haplorrhini, and perhaps explains why previous studies recovered conflicting resolutions for the placement of tarsiers [31,64,65].

The remaining branches of the species tree that define major primate clades all have remarkably high concordance with the underlying gene trees (gCF > 80%), though individual branches within these clades do not. The gCFs for the branches defining these clades are: Strepsirrhini (lemurs+lorises) = 84.5, Catarrhini (OWM+Apes) = 90.0, Platyrrhini (NWM) = 96.6, Hominoidea (Apes) = 82.7, and Cercopithecidae (OWM) = 92.3 (Figure 1). High gene tree/species tree concordance for these branches is likely due to a combination of more recent divergences (increasing gene tree accuracy) and longer times between branching events [66]. Within these clades, however, we see multiple recent radiations. One of the most contentious has been among the New World Monkeys, a set of relationships we address next.

Concatenation Affects Resolution of the New World Monkey Radiation

Sometime during the mid-to-late Eocene (~45-34 mya), a small number of primates arrived on the shores of South America [15,67]. These monkeys likely migrated from Africa [67] and on arrival underwent multiple rounds of extinction and diversification [15], the most recent of which was aided by a period of warming referred to as the Mid-Miocene Climatic Optimum [59]. Three extant families from this radiation now make up the New World Monkeys (Platyrrhini, Figure 1). Because of the rapidity with which these species spread and diversified across the new continent, relationships at the base of the NWM have been hard to determine [12–14,16–18].

As reported above, the concatenated analysis (ML-CONCAT) gives a different topology than the gene tree-based analysis (ML-ASTRAL). Specifically, the ML-CONCAT analysis supports a symmetrical tree, with *Aotus* sister to *Callithrix* (Figure

2A). In contrast, ML-ASTRAL supports an asymmetrical (or "caterpillar") tree, with *Aotus* sister to a clade comprised of *Saimiri*+*Cebus* (Figure 2B). There are reasons to have doubts about both topologies. It is well known that carrying out maximum likelihood analyses of concatenated datasets can result in incorrect species trees, especially when the time between speciation events is short [68,69]. In fact, the specific error that is made in these cases is for ML concatenation methods to prefer a symmetrical four-taxon tree over an asymmetrical one, exactly as is observed here. Gene tree-based methods such as ASTRAL are not prone to this particular error, as long as the underlying gene trees are all themselves accurate [70,71]. However, if there is bias in gene tree reconstruction, then there are no guarantees as to the accuracy of the species tree. In addition, the ML-ASTRAL tree is supported by only a very small plurality of gene trees: there are 442 trees supporting this topology, compared to 437 supporting the ML-CONCAT topology and 413 supporting the third topology (Figure 2D). This small excess of supporting gene trees also explains the relatively low posterior support for this branch in the species tree (Figure 1). Additionally, a polytomy test [72], implemented in ASTRAL and performed using ML gene trees, failed to reject the null hypothesis of "polytomy" for the branch uniting *Aotus*+(*Saimiri,Cebus*) (P=0.47).

To investigate these relationships further, we carried out additional analyses. The trees produced from concatenated alignments are biased when maximum likelihood is used for inference, but this bias does not affect parsimony methods [21,73]. Therefore, we analyzed exactly the same concatenated 1.76 Mb alignment used as input for ML, but carried out a maximum parsimony analysis in PAUP* [74]. As would be expected given the known biases of ML methods, the maximum parsimony tree (which we refer to

as “MP-CONCAT”) returns the same tree as ML-ASTRAL, supporting an asymmetric topology of NWMs (Figure 2B). Underlying this result is a relatively large excess of parsimony-informative sites supporting this tree (Figure 2F), which results in maximal bootstrap values for every branch. The two most diverged species in this clade (*Saimiri* and *Callithrix*) are only 3.26% different at the nucleotide level, so there should be little effect of multiple substitutions on the parsimony analysis.

As mentioned above, gene tree-based methods (such as ASTRAL) are not biased when accurate gene trees are used as input. However, in our initial analyses we used maximum likelihood to infer the individual gene trees. Because protein-coding genes are themselves often a combination of multiple different underlying topologies [75], ML gene trees may be biased, and using them as input to gene tree-based methods may still lead to incorrect inferences of the species tree [76]. Therefore, we used the same 1,730 loci as above to infer gene trees using maximum parsimony with MPBoot [77]. Although the resulting topologies still possibly represent the average over multiple topologies contained within a protein-coding gene, using parsimony ensures that this average tree is not a biased topology. These gene trees were used as input to estimate a species tree using ASTRAL; we refer to this as the “MP-ASTRAL” tree. Once again, the methods that avoid known biases of ML lend further support to an asymmetric tree, placing *Aotus* sister to the *Saimiri*+*Cebus* clade (Figure 2B). In fact, the gene trees inferred with parsimony now show a much greater preference for this topology, with a clear plurality of gene trees supporting the species tree (473 vs. 417 supporting the second-most common tree; Figure 2E). As a consequence, the local posterior for this branch in the MP-ASTRAL tree is 0.92 and the polytomy test

291 performed using MP gene trees rejects (p = 0.037) the null hypothesis of "polytomy" for
292 the branch uniting *Aotus*+(*Saimiri,Cebus*). The increased number of concordant gene
293 trees using parsimony suggests that the gene trees inferred using ML may well have
294 been suffering from the biases of concatenation within each locus, reducing the
295 observed levels of concordance.

296 A recent analysis of NWM genomes found *Aotus* sister to *Callithrix*, as in the ML-
297 CONCAT tree, despite the use of gene trees to build the species tree [18]. However, the
298 outgroup used in this analysis is a closely related species (*Brachyteles arachnoides*)
299 that diverged during the NWM radiation and that shares a recent common ancestor with
300 the ingroup taxa [12,13]. If the outgroup taxon used to root a tree shares a more recent
301 common ancestor with subsets of ingroup taxa at an appreciable number of loci, the
302 resulting tree topologies will be biased. A similar problem likely arose in previous
303 studies that have used the Scandentia or Dermoptera as outgroups to Primates. In
304 general, this issue highlights the difficulty in choosing outgroups: though we may have
305 100% confidence that a lineage lies outside our group of interest in the species tree, a
306 reliable outgroup must also not have any discordant gene trees that place it inside the
307 ingroup.

308 **Strongly Supported Divergence Times Using Fossil Calibrations**

309 Fossil-constrained molecular dating was performed using 10 independent
310 datasets, each of which consisted of 40 protein-coding genes randomly selected
311 (without replacement) and concatenated. The resulting datasets had an average
312 alignment length of 39,374 bp (SD=2.6x10^3, Table S4). Although individual discordant

trees included in this analysis may have different divergence times, the difference in estimates of dates should be quite small [78]. We used eight dated fossils (blue stars in Figure 1) from 10 studies for calibration (Table S5). The most recent of these fossils is ~5.7 mya [79], while the most ancient is 55.8 mya [80]. Each separate dataset and the same set of "soft" fossil constraints, along with the species tree in Figure 1, were used as input to PhyloBayes 3.3 [81] which was run twice to assess convergence (Materials and Methods).

We observed tight clustering of all estimated node ages across datasets and independent runs of PhyloBayes (Figure 3 and Table S6). In addition, the ages of most major crown nodes estimated here are largely in agreement with previously published age estimates (Table 2). Some exceptions include the age of the crown Strepsirrhini (47.4 mya) and Haplorrhini (59.0 mya) which are more recent than many previous estimates for these nodes (range in the literature is Strepsirrhini = 51.6 - 68.7, Haplorrhini = 60.6 – 81.3). The crown nodes for Catarrhini, Hominoidea, and Cercopithecidae (28.4, 21.4, and 16.8 mya, respectively) all fall within the range of variation recovered in previous studies (Table 2).

Our estimate for the most recent common ancestor of the extant primates (i.e. the last common ancestor of Haplorrhini and Strepsirrhini) is 61.7 mya, which is slightly more recent than several studies [13,31,33,82] and much more recent than other studies [12,83,84]. However, our estimate is in good agreement with Herrera *et al.* [32], who used 34 fossils representing extinct and extant lineages (primarily Strepsirrhines) to infer divergence times among primates, concluding that the split occurred approximately 64 mya. One similarity between our study and that of Herrera *et al.* is that we have both

used the maximum constraint of 65.8 my on the ancestral primate node suggested by Benton *et al.* [85], which likely contributes to the more recent divergence. It is worth noting that the soft bounds imposed in our analysis permit older ages to be sampled from the Markov chain, but these represented only a small fraction (median 3.37%) of the total sampled states after burn-in (Table S5). To determine the effects of imposing the 65.8 my maximum constraint on the Primate node, we analyzed all 10 datasets for a third time with this constraint removed and report the divergence time of major primate clades in Table 2 ("No Max" entries).

There are several caveats to our age estimates that should be mentioned. Maximum age estimates for the crown node of any given clade are defined by the oldest divergence among sampled taxa in the clade. This limitation results in underestimates for nearly all crown node ages as, in practice, complete taxon sampling is difficult to achieve. Fossil calibrations are often employed as minimum constraints in order to overcome the limitations imposed by taxon sampling, allowing older dates to be estimated more easily. On the other hand, the systematic underestimation of crown node ages due to taxon sampling is somewhat counteracted by the overestimation of speciation times due to ancestral polymorphism. Divergence times estimated from sequence data represent the coalescence times of sequences, which are necessarily older than the time at which two incipient lineages diverged [86,87]. This overestimation will have a proportionally larger effect on recent nodes (such as the *Homo/Pan* split; Figure 3, node 15), but the magnitude can be no larger than the average level of polymorphism in ancestral populations and will be additionally reduced by post-divergence gene flow.

359 **Introgression During the Radiation of Primates**

360 There is now evidence for recent inter-specific gene flow between many extant
361 primates, including introgression events involving humans [24], gibbons [88,89],
362 baboons [9,27], macaques [90,91], and vervet monkeys [10], among others. While there
363 are several widely used methods for detecting introgression between closely related
364 species (see chapters 5 and 9 in [92]), detecting ancient gene flow is more difficult. One
365 of the most popular methods for detecting recent introgression is the *D* test (also known
366 as the "ABBA-BABA" test; [93]). This test is based on the expectation that, for any given
367 branch in a species tree, the two most frequent alternative resolutions should be
368 present in equal proportions. However, the *D* test uses individual SNPs to evaluate
369 support for alternative topologies, and explicitly assumes an infinite sites model of
370 mutation (i.e. no multiple hits). As this assumption will obviously not hold the further
371 back in time one goes, a different approach is needed.

372 Fortunately, Huson *et al*. [36] described a method that uses gene trees
373 themselves (rather than SNPs) to detect introgression. Using the same expectations as
374 in the *D* test, these authors looked for a deviation from the expected equal numbers of
375 alternative tree topologies using a test statistic they refer to as Δ. As far as we are
376 aware, Δ has only rarely been used to test for introgression in empirical data, possibly
377 because of the large number of gene trees needed to assess significance, or the
378 assumptions of the parametric method proposed to obtain *P*-values. Here, given our
379 large number of gene trees and large number of internal branches to be tested, we
380 adapt the Δ test for genome-scale data.

To investigate patterns of introgression within primates, we used 1,730 single-copy loci to test for deviations from the null expectation of Δ on each of the 24 internal branches of the primate phylogeny (Materials and Methods). To test whether deviations in Δ were significant (i.e. $\Delta > 0$), we generated 2000 resampled datasets of 1,730 gene tree topologies each. *P*-values were calculated from *Z*-scores generated from these resampled datasets. Among the 17 branches where at least 5% of topologies were discordant, we found 7 for which Δ had $P<0.05$.

To further verify these instances of potential introgression, for each of these seven branches we increased the number of gene trees used by subsampling a smaller set of taxa. We randomly chose four taxa for each internal branch tested that also had this branch as an internal branch, and then re-aligned orthologs present in a single copy in each taxon. These steps resulted in ~3,600-6,400 genes depending on the branch being tested (Supplementary Table S7). Additionally, because instances of hybridization and introgression are well documented among macaques [90,91,94], we similarly re-sampled orthologs from the three *Macaca* species in our study.

We recalculated Δ using the larger gene sets and found significant evidence (after correcting for m=17 multiple comparisons by using a cutoff of $P = 0.00301$) for six introgression events, all of which occurred among the Papionini (Figure 4 and see next paragraph). Within the Hominoidea, we found $\Delta = 0.0518$ for the branch leading to the great apes, but $P = 0.030$. The asymmetry in gene tree topologies here suggests gene flow may have happened between gibbons (represented by *Nomascus*) and the ancestral branch leading to the African hominoids (humans, chimpanzees, and gorillas),

but, like the *D* test, Δ cannot tell us the direction of introgression. Although currently separated by significant geographic distances (African apes south of the Sahara Desert and gibbons all in southeast Asia), it is worth noting that fossil hominoids dating from the early to late Miocene had a broad distribution extending from southern Africa to Europe and Asia [95]. Support for introgression between ancestral hominins and ancestral chimpanzees has been previously reported [96]; our four-taxon analyses found marginal support for this conclusion (Δ = 0.0917, *P* = 0.055).

Within the OWM, ~40% of Cercopithicine species are known to hybridize in nature [34]. Consistent with this, *Macaca nemestrina* and *M. fascicularis* showed a strong signature of gene flow in our data (Δ = 0.1761, *P* = 1.377e-09). These two species have ranges that currently overlap (Figure S1). In contrast to the clear signal of recent gene flow in the macaques, we detected a complex pattern of ancient introgression between the African Papionini (*Cercocebus, Mandrillus, Papio, and Theropithecus*) and the Asian Papionini (*Macaca*) (Figure 4). The Δ test was significant using multiple different subsamples of four taxa, suggesting multiple ancestral introgression events. An initial attempt to disentangle these events using Phylonet v3.8.0 [97,98] with the seven Papionini species and an outgroup was unsuccessful, as Phylonet failed to converge on an optimal network for these taxa. When there are multiple episodes of gene flow within a clade, even complex computational machinery may be unable to infer the correct combination of events.

As an alternative approach, we used four-taxon trees to estimate Δ for each *Macaca* species paired with two African Papionini (one from the *Papio*+*Theropithecus* clade and one from the *Mandrillus* +*Cercocebus* clade; see Table S7) and an outgroup.

Significant introgression was detected using each of the *Macaca* species and three of the four African Papionini species (*Cercocebus, Theropithecus,* and *Papio*). These results suggest gene flow between the ancestor of the three *Macaca* species in our analysis and the ancestors of the three African Papionini in our analysis, or one introgression event involving the ancestor of all four African species coupled with a second event that masked this signal in *Mandrillus*. This second event may either have been biological (additional introgression events masking the signal), or technical (possibly the lack of continuity or completeness of the *Mandrillus* reference genome sequence), but in either case we could not detect introgression in the available drill sequence. The latter scenario would fit better with the current geographic distributions of these species, as they are on two different continents. However, the fossil record indicates that by the late Miocene to late Pleistocene the ancestral distribution of the genus *Macaca* covered all of North Africa, into the Levant, and as far north as the U.K. (Figure S1; [99]). The fossil record for *Theropithecus* indicates several species had distributions that overlapped with *Macaca* during this time, including in Europe and as far east as India (Figure S1, [100,101]). Ancestral macaques and ancestral papionins may therefore have come into contact in the area of the Mediterranean Sea. The Sahara Desert is also responsible for the current disjunct distributions of many of these species. However, this region has experienced periods of increased rainfall or "greenings" over the past several million years [102–104]. Faunal migration through the Sahara, including by hominins, is hypothesized to have occurred during these green periods [103,105,106] resulting in successive cycles of range expansion and contraction

448 [107]. Hybridization and introgression could have occurred between the ancestors of
449 these groups during one of these periods.

450 Our results on introgression come with multiple caveats, both about the events
451 we detected and the events we did not detect. As with the *D* test, there are multiple
452 alternative explanations for a significant value of Δ besides introgression. Ancestral
453 population structure can lead to an asymmetry in gene tree topologies [108] though it
454 requires a highly specific, possibly unlikely population structure. For instance, if the
455 ancestral population leading to *Macaca nemestrina* was more closely related to *M.*
456 *fascicularis* than was the ancestral population leading to its sister species, *M. mulatta*
457 (Figure 4), then there could be an unequal number of alternative topologies. Similarly,
458 any bias in gene tree reconstruction that favors one alternative topology over the other
459 could potentially lead to a significant value of Δ. While this scenario is unlikely to affect
460 recent divergences using SNPs, well known biases that affect topology reconstruction
461 deeper in the tree (such as long-branch attraction) could lead to gene tree asymmetries.
462 However, we did not observe any significant Δ-values for branches more than ~10 my
463 old.

464 There are also multiple reasons why our approach may have missed
465 introgression events, especially deeper in the tree. All methods that use asymmetries in
466 gene tree topologies miss gene flow between sister lineages, as such events do not
467 lead to changes in the proportions of underlying topologies. Similarly, equal levels of
468 gene flow between two pairs of non-sister lineages can mask both events, while even
469 unequal levels will lead one to miss the less-frequent exchange. More insidiously,
470 especially for events further back in time, extinction of the descendants of hybridizing

lineages will make it harder to detect introgression. Internal branches closer to the root will be on average longer than those near the tips because of extinction [109], and therefore introgression between non-sister lineages would have to occur longer after speciation in order to be detected. For instance, gene flow among Strepsirrhine species has been detected in many previous analyses of more closely related species (e.g. [110–113]) but the deeper relationships among the taxa sampled here may have made it very difficult to detect introgression. Nevertheless, our analyses were able to detect introgression between many primate species across the phylogeny.

Conclusions

Several previous phylogenetic studies of primates have included hundreds of taxa, but fewer than 70 loci [12,13]. While the species tree topologies produced by these studies are nearly identical to the one recovered in our analysis, the limited number of loci meant that it was difficult to assess gene tree discordance accurately. By estimating gene trees from 1,700 single-copy loci, we were able to assess the levels of discordance present at each branch in the primate phylogeny. Understanding discordance helps to explain why there have been longstanding ambiguities about species relationships near the base of primates and in the radiation of New World Monkeys. Our analyses reveal how concatenation of genes—or even of exons—can mislead maximum likelihood phylogenetic inference in the presence of discordance, but also how to overcome the biases introduced by concatenation in some cases. Discordance also provides a window into introgression among lineages, and here we have found evidence for exchange among several species pairs. Each instance of

493 introgression inferred from the genealogical data is plausible insofar as it can be
494 reconciled with current and ancestral species distributions.

495 Materials and Methods

496 Source Material and Sequencing

497 For the sequencing of the *Colobus angolensis palliatus* genome, paired-end (100
498 bp) libraries were prepared using DNA extracted from heart tissue (isolate OR3802)
499 kindly provided by Dr. Oliver Ryder (San Diego Zoo). Sequencing was performed using
500 nine Illumina Hi-seq 2000 lanes and four Illumina Hi-seq 2500 lanes with subsequent
501 assembly carried out using ALLPATHS-LG software (v. 48744) [114]. Additional
502 scaffolding and gap-filling was performed using Atlas-Link v. 1.1
503 (https://www.hgsc.bcm.edu/software/atlas-link) and Atlas-GapFill v. 2.2.
504 (https://www.hgsc.bcm.edu/software/atlas-gapfill) respectively. Annotation for all three
505 species was carried out using the NCBI Eukaryotic Genome Annotation Pipeline. A
506 complete description of the pipeline can be viewed at
507 https://www.ncbi.nlm.nih.gov/genome/annotation_euk/process/.
508 For the sequencing of the *Macaca nemestrina* genome, DNA was extracted from
509 a blood sample (isolate M95218) kindly provided by Dr. Betsy Ferguson and Dr. James
510 Ha (Washington National Primate Research Center). Paired-end libraries were prepared
511 and sequenced on 20 Illumina Hi-Seq 2000 lanes with the initial assembly performed
512 using ALLPATHS-LG as above. Scaffolding was conducted using Atlas-Link v. 1.1.
513 Additional gap-filling was performed using the original Illumina reads and Atlas-GapFill
514 v. 2.2, as well as long reads generated using the Pacific Biosciences RS (60 SMRT

cells) and RSII (50 SMRT cells) platforms. The PacBio reads were mapped to scaffolds to fill remaining gaps in the assembly using PBJelly2 (v. 14.9.9) [115].

For the sequencing of the *Mandrillus leucophaeus* genome, DNA was extracted from heart tissue (isolate KB7577) kindly provided by Dr. Oliver Ryder (San Diego Zoo). Paired-end libraries were prepared and sequenced on nine Illumina Hi-Seq 2000 lanes with the initial assembly performed using ALLPATHS-LG as above. Additional scaffolding was completed using Atlas-Link v. 1.1 and additional gap-filling in scaffolds was performed using the original Illumina reads and Atlas-GapFill v. 2.2.

Phylogenomic Analyses

The full set of protein-coding genes for 26 primates and 3 non-primates were obtained by combining our newly sequenced genomes with already published data (see Table S1 for references and accessions and Tables 1 and S2 for genome statistics). Ortholog clustering was performed by first executing an all-by-all BLASTP search [116,117] using the longest isoform of each protein coding gene from each species. The resulting BLASTP output was clustered using the mcl algorithm [118] as implemented in FastOrtho [119] with various inflation parameters (the maximum number of clusters was obtained with *inflation=5*). Orthogroups were then parsed to retain those genes present as a single-copy in all 29 taxa (1,180 genes), 28 of 29 taxa (1,558 genes), and 27 of 29 taxa (1,735 genes). We chose to allow up to two missing species per alignment to maximize the data used in our phylogenomic reconstructions while maintaining high taxon-occupancy in each alignment. Coding sequences (CDS) for each single-copy orthogroup were aligned, cleaned, and trimmed via a multi-step process: First,

sequences in each orthogroup were aligned by codon using GUIDANCE2 [120] in conjunction with MAFFT v7.407 [121] with 60 bootstrap replicates. Sequence residues in the resulting MAFFT alignment with GUIDANCE scores < 0.93 were converted to gaps and sites with > 50% gaps were removed using Trimal v1.4.rev22 [122]. Alignments shorter than 200 bp (full dataset) or 300 bp (four-taxon tests for introgression), and alignments that were invariant or contained no parsimony informative characters, were removed from further analyses. This resulted in 1,730 loci for the full analysis (see Table S7 for gene counts used in four-taxon tests).

IQ-TREE v2-rc1 was used with all 1,730 aligned loci to estimate a maximum likelihood concatenated (ML-CONCAT) tree with an edge-linked, proportional-partition model and 1,000 ultrafast bootstrap replicates [39,123,124]. The full IQ-TREE commandline used was: “iqtree -p Directory_of_Gene_Alignments --prefix -m MFP -c 8 -B 1000”. Maximum likelihood gene trees were estimated for each alignment with nucleotide substitution models selected using ModelFinder [125] as implemented in IQ-TREE. The full IQ-TREE commandline used was: “iqtree -s Directory_of_Gene_Alignments --prefix -m MFP -c 8”. We used the resulting maximum likelihood gene trees to estimate a species tree using ASTRAL III (ML-ASTRAL) [38]. Parsimony gene trees were generated using MPboot [77] and used to estimate a species tree using ASTRAL III (MP-ASTRAL), while PAUP* [74] was used to estimate the concatenated parsimony tree (MP-CONCAT) with 500 bootstrap replicates. IQ-TREE was used to calculate both gene concordance factors (gCFs) and site concordance factors (sCFs), with sCFs estimated from 300 randomly sampled quartets

using the commandline: “iqtree --cf-verbose --gcf 1730_GENETREE.treefile -t Species_tree_file --df-tree --scf 300 -p Directory_of_Gene_Alignments -c 4”.

Introgression Analyses

For each internal branch of the Primate tree where the proportion of discordant trees was > 5% of the total, concordance factors were used to calculate the test statistic Δ, where:

$$\Delta = \frac{Number\ of\ DF1\ trees - Number\ of\ DF2\ trees}{Number\ of\ DF1\ trees + Number\ of\ DF2\ trees}$$

Where *DF1* trees represent the most frequent discordant topology and *DF2* trees are the second most frequent discordant topology. This is a normalized version of the statistic proposed by Huson *et al.* [36], which only included the numerator of this expression. Note also that, by definition, Δ here is always equal to or greater than 0. To test whether deviations from zero were significant (i.e. $\Delta > 0$), we calculated Δ for 2,000 pseudo-replicate datasets generated by resampling gene trees with replacement. The resulting distribution was used to calculate *Z*-scores and the resulting *P*-values for the observed Δ value associated with each branch tested [126]. Of the 17 internal branches where > 5% of topologies were discordant, 7 were significant at $P < 0.05$, and selected for more extensive testing. For each of the 7 significant branches in the all-Primates tree, 4 taxa were selected that included the target branch as an internal branch. Single-copy genes present in each taxon were aligned as previously described. Alignments with no variant or parsimony-informative sites were removed from the analysis and gene trees were estimated using maximum likelihood in IQ-TREE 2. The test statistic, Δ, was

580 calculated and significance was again determined using 2,000 bootstrap replicates with
581 the *P*-value threshold for significance corrected for multiple comparisons (*m*=17) using
582 the Dunn–Šidák correction [127,128].

583 **Molecular Dating**

584 Molecular dating analyses were performed on 10 datasets consisting of 40 CDS
585 alignments each sampled randomly without replacement from the 1,730 loci used to
586 estimate the species tree. Gene alignments were concatenated into 10 supermatrices
587 ranging from 36.7 kb – 42.7 kb in length (see Table S4 for the length of each
588 alignment). Each dataset was then analyzed using PhyloBayes 3.3 [81] with sequences
589 modeled using a site-specific substitution process with global exchange rates estimated
590 from the data (CAT-GTR; [129]). Among-site rate-variation was modeled using a
591 discrete gamma distribution with six rate categories. A relaxed molecular clock [130]
592 with eight, soft-bounded, fossil calibrations (see Table S5) was used to estimate
593 divergence times on the fixed species tree topology (Figure 1), the analyses were
594 executed using the following command line: pb -x 1 15000 -d Alignment.phy -T
595 Tree_file.tre -r outgroup_file.txt -cal 8_fossil.calib -sb -gtr -cat -bd -dgam 6 -ln -rp 90 90.
596 Each dataset was analyzed for 15,000 generations, sampling every 10 generations, with
597 5,000 generations discarded as burn-in. Each dataset was analyzed twice to ensure
598 convergence of the average age estimated for each node (Figure 3 shows the node age
599 for both runs). To determine the effect of including a maximum constraint on the root of
600 the Primates, we analyzed each dataset a third time with this constraint removed. Both
601 the constrained and unconstrained node ages for major groups within the Primates are
602 reported in Table 2.

603

604 Acknowledgements

605 We thank Yue Liu for assistance in assembling the genomes, and Fábio Mendes and
606 Gregg Thomas for helpful advice. This work was supported by National Science
607 Foundation grants DBI-1564611 and DEB-1936187 (M.W.H), a Chan-Zuckerberg
608 Initiative grant for Essential Open Source Software for Science (B.Q.M. and R.L.), and
609 Australian Research Council grant DP-200103151 (R.L., B.Q.M., and M.W.H.).

610

Tables

Species name	Assembly Accession	Assembly Total length	Number of scaffolds	Scaffold N50	Number of contigs	Protein-coding genes	BUSCO
Colobus angolensis ssp. palliatus (the black and white colobus)	GCF_000951035.1	2,970,124,662	13,124	7,840,981	197,124	20,222	95.82%
Macaca nemestrina (pig-tailed macaque)	GCF_000956065.1	2,948,703,511	9,733	15,219,753	94,057	21,017	95.98%
Mandrillus leucophaeus (drill)	GCF_000951045.1	3,061,992,840	12,821	3,186,748	246,054	20,465	95.45%

Table 1.

Genomes sequenced in this study and associated assembly and annotation metrics. BUSCO percentages reflect the complete and fragmented genes relative to the Euarchontoglires ortholog database v9.

Table 2.

Node	This Study	This Study No Max*	Herrera *et al.* [32]	Kistler *et al.* [33]	Perez *et al.* [17]	Springer *et al.* [13]	Meredith *et al.* [45]	Perelman *et al.* [12]	Wilkinson *et al.* [83]	Chatterjee *et al.* [31]
Primates	61.7	67.5	63.9	68	NA	67.8	71.5	87.2	84.5	63.7
Strepsirrhini	47.4	50.2	61.4	59	NA	54.2	55.1	68.7	49.8	51.6
Haplorrhini	59.0	63.8	61.9	67	60.6	61.2	62.4	81.3	NA	NA
Catarrhini	28.4	29.0	32.1	33	27.8	25.1	20.6	31.6	31.0	29.3
Hominoidea	21.4	21.6	NA	21	18.44	17.4	14.4	20.3	NA	21.5
Cercopithecidae	16.8	16.9	NA	24	13.4	13.2	NA	17.6	14.1	23.4

Mean crown node divergence times estimated in this study compared with mean divergences times estimated by eight prior studies. Estimates were calculated by averaging the mean times across all runs for 10 independent datasets.
*Refers to the average divergence time of the crown node for the indicated taxonomic group when the 65.8 my maximum constraint was removed from the Primate node.

Figure Legends

Figure 1. Species tree estimated using ASTRAL III with 1,730 gene trees (the *Mus musculus* outgroup was removed to allow for a visually finer scale). Common names for each species can be found in Table S1. Node labels indicate the bootstrap value from a maximum likelihood analysis of the concatenated dataset as well as the local posterior probability from the ASTRAL analysis. Gene concordance factors (gCF) and site concordance factors (sCF) are also reported. Eight fossil calibrations (blue stars; Table S5) were used to calibrate node ages. Grey bars indicate the minimum and maximum mean age from independent dating estimates. The inset tree with colored branches shows the maximum likelihood branch lengths estimated using a partitioned analysis of the concatenated alignment. Colors correspond to red = Strepsirrhini, cyan = Tarsiiformes, green = Platyrrhini (New World Monkeys), blue = Cercopithecoidea (Old World Monkeys), orange = Hominoidea (Apes).

Figure 2. The three most frequent topologies of New World Monkeys. A) Tree 1 is the symmetrical topology inferred by the maximum likelihood concatenated analysis (ML-CONCAT) of 1,730 loci (1.76 Mb). B) Tree 2 is the asymmetrical topology inferred by ASTRAL III using either maximum likelihood (ML-ASTRAL) or maximum parsimony (MP-ASTRAL) gene tree topologies. Using maximum parsimony on the concatenated alignment also returns this tree (MP-CONCAT). C) Tree 3 is the alternative resolution recovered at high frequency in all gene tree analyses, though it is not the optimal species tree using any of the methods. D) Number of gene trees supporting each of the three resolutions of the NWM clade when maximum likelihood is used to infer gene tree

topologies. There are 1,637 decisive gene trees for these splits. E) Gene tree counts when maximum parsimony is used to infer gene tree topologies. F) Number of parsimony informative sites in the concatenated alignment supporting each of the three resolutions.

Figure 3. Mean node ages for independent Phylobayes dating runs on 10 different datasets (each dataset was run twice). Box plots show the median, interquartile range, and both minimum and maximum values of the mean nodes ages. An additional run was performed with no sequence data to ascertain the prior on node divergence times in the presence of fossil calibrations (pink asterisks). Some prior ages were too large to include in the plot while still maintaining detail; these ages are given as numeric values. The species tree topology is from Figure 1, 95% highest posterior density (HPD) intervals for each node are reported in Table S6.

Figure 4. Introgression among Papionini taxa (the species tree is unrooted for clarity). Arrows indicate that a significant Δ was found in our four taxon tests and identify the two lineages inferred to have exchanged genes (values underlying these tests are listed in Table S7). Among the Papionini, there was evidence of introgression between African taxa (*Papio*, *Theropithecus*, and *Cercocebus*) and Asian *Macaca* species (light grey arrows). Introgression events likely occurred between African taxa and the ancestral *Macaca*, which had a wide distribution across northern Africa prior to the radiation throughout Asia 2-3 mya [131]. More recent instances of introgression are inferred between macaque species and among the African Papionini (dark grey arrows).

669 # References

670 1. The 1000 Genomes Project Consortium. A map of human genome variation from
671 population-scale sequencing. Nature. 2011;473: 544–544.
672 doi:10.1038/nature09991

673 2. Fawcett GL, Raveendran M, Deiros DR, Chen D, Yu F, Harris RA, et al.
674 Characterization of single-nucleotide variation in Indian-origin rhesus macaques
675 (*Macaca mulatta*). BMC Genomics. 2011;12: 311. doi:10.1186/1471-2164-12-311

676 3. Higashino A, Sakate R, Kameoka Y, Takahashi I, Hirata M, Tanuma R, et al.
677 Whole-genome sequencing and analysis of the Malaysian cynomolgus macaque
678 (*Macaca fascicularis*) genome. Genome Biol. 2012;13: R58. doi:10.1186/gb-2012-
679 13-7-r58

680 4. Kuhlwilm M, Han S, Sousa VC, Excoffier L, Marques-Bonet T. Ancient admixture
681 from an extinct ape lineage into bonobos. Nat Ecol Evol. 2019;3: 957–965.
682 doi:10.1038/s41559-019-0881-7

683 5. Locke DP, Hillier LW, Warren WC, Worley KC, Nazareth LV, Muzny DM, et al.
684 Comparative and demographic analysis of orang-utan genomes. Nature.
685 2011;469: 529–533. doi:10.1038/nature09687

686 6. de Manuel M, Kuhlwilm M, Frandsen P, Sousa VC, Desai T, Prado-Martinez J, et
687 al. Chimpanzee genomic diversity reveals ancient admixture with bonobos.
688 Science. 2016;354: 477–481. doi:10.1126/science.aag2602

689 7. Prado-Martinez J, Sudmant PH, Kidd JM, Li H, Kelley JL, Lorente-Galdos B, et al.
690 Great ape genetic diversity and population history. Nature. 2013;499: 471–475.
691 doi:10.1038/nature12228

692 8. Prüfer K, Munch K, Hellmann I, Akagi K, Miller JR, Walenz B, et al. The bonobo
693 genome compared with the chimpanzee and human genomes. Nature. 2012;486:
694 527–531. doi:10.1038/nature11128

695 9. Rogers J, Raveendran M, Harris RA, Mailund T, Leppälä K, Athanasiadis G, et al.
696 The comparative genomics and complex population history of *Papio* baboons. Sci
697 Adv. 2019;5: eaau6947. doi:10.1126/sciadv.aau6947

698 10. Svardal H, Jasinska AJ, Apetrei C, Coppola G, Huang Y, Schmitt CA, et al.
699 Ancient hybridization and strong adaptation to viruses across African vervet
700 monkey populations. Nat Genet. 2017;49: 1705–1713. doi:10.1038/ng.3980

701 11. Zhou X, Wang B, Pan Q, Zhang J, Kumar S, Sun X, et al. Whole-genome
702 sequencing of the snub-nosed monkey provides insights into folivory and
703 evolutionary history. Nat Genet. 2014;46: 1303–1310. doi:10.1038/ng.3137

12. Perelman P, Johnson WE, Roos C, Seuánez HN, Horvath JE, Moreira MAM, et al. A molecular phylogeny of living primates. PLOS Genet. 2011;7: e1001342. doi:10.1371/journal.pgen.1001342

13. Springer MS, Meredith RW, Gatesy J, Emerling CA, Park J, Rabosky DL, et al. Macroevolutionary dynamics and historical biogeography of primate diversification inferred from a species supermatrix. PLOS One. 2012;7: e49521. doi:10.1371/journal.pone.0049521

14. Wang X, Lim BK, Ting N, Hu J, Liang Y, Roos C, et al. Reconstructing the phylogeny of new world monkeys (Platyrrhini): evidence from multiple non-coding loci. Curr Zool. 2019;65: 579–588. doi:10.1093/cz/zoy072

15. Silvestro D, Tejedor MF, Serrano-Serrano ML, Loiseau O, Rossier V, Rolland J, et al. Early arrival and climatically-linked geographic expansion of New World monkeys from tiny African ancestors. Syst Biol. 2018;68: 78–92. doi:10.1093/sysbio/syy046

16. Jameson Kiesling NM, Yi SV, Xu K, Gianluca Sperone F, Wildman DE. The tempo and mode of New World monkey evolution and biogeography in the context of phylogenomic analysis. Mol Phylogenet Evol. 2015;82 Pt B: 386–399. doi:10.1016/j.ympev.2014.03.027

17. Perez SI, Tejedor MF, Novo NM, Aristide L. Divergence times and the evolutionary radiation of New World monkeys (Platyrrhini, Primates): an analysis of fossil and molecular data. PLOS One. 2013;8: e68029. doi:10.1371/journal.pone.0068029

18. Schrago CG, Seuánez HN. Large ancestral effective population size explains the difficult phylogenetic placement of owl monkeys. Am J Primatol. 2019;55: e22955. doi:10.1002/ajp.22955

19. Degnan JH, Rosenberg NA. Discordance of species trees with their most likely gene trees. PLOS Genet. 2006;2: e68. doi:10.1371/journal.pgen.0020068

20. Huang H, Knowles LL. What is the danger of the anomaly zone for empirical phylogenetics? Syst Biol. 2009;58: 527–536. doi:10.1093/sysbio/syp047

21. Mendes FK, Hahn MW. Why concatenation fails near the anomaly zone. Syst Biol. 2018;67: 158–169. doi:10.1093/sysbio/syx063

22. Mallet J. Hybridization as an invasion of the genome. Trends Ecol Evol. 2005;20: 229–237. doi:10.1016/j.tree.2005.02.010

23. Mallet J, Besansky N, Hahn MW. How reticulated are species? BioEssays. 2016;38: 140–149. doi:10.1002/bies.201500149

24. Green RE, Krause J, Briggs AW, Maricic T, Stenzel U, Kircher M, et al. A draft sequence of the Neandertal genome. Science. 2010;328: 710–722. doi:10.1126/science.1188021

25. Lima MGM, Silva-Júnior J de SE, Černý D, Buckner JC, Aleixo A, Chang J, et al. A phylogenomic perspective on the robust capuchin monkey (*Sapajus*) radiation: First evidence for extensive population admixture across South America. Mol Phylogenet Evol. 2018;124: 137–150. doi:10.1016/j.ympev.2018.02.023

26. de Manuel M, Kuhlwilm M, Frandsen P, Sousa VC, Desai T, Prado-Martinez J, et al. Chimpanzee genomic diversity reveals ancient admixture with bonobos. Science. 2016;354: 477–481. doi:10.1126/science.aag2602

27. Wall JD, Schlebusch SA, Alberts SC, Cox LA, Snyder-Mackler N, Nevonen KA, et al. Genomewide ancestry and divergence patterns from low-coverage sequencing data reveal a complex history of admixture in wild baboons. Mol Ecol. 2016;25: 3469–3483. doi:10.1111/mec.13684

28. Huerta-Sanchez E, Jin X, Asan, Bianba Z, Peter BM, Vinckenbosch N, et al. Altitude adaptation in Tibetans caused by introgression of Denisovan-like DNA. Nature. 2014;512: 194–197. doi:10.1038/nature13408

29. Racimo F, Sankararaman S, Nielsen R, Huerta-Sanchez E. Evidence for archaic adaptive introgression in humans. Nat Rev Genet. 2015;16: 359–371. doi:10.1038/nrg3936

30. Racimo F, Gokhman D, Fumagalli M, Ko A, Hansen T, Moltke I, et al. Archaic adaptive introgression in *TBX15/WARS2.* Mol Biol Evol. 2017;34: 509–524. doi:10.1093/molbev/msw283

31. Chatterjee HJ, Ho SYW, Barnes I, Groves C. Estimating the phylogeny and divergence times of primates using a supermatrix approach. BMC Evol Biol. 2009;9: 259. doi:10.1186/1471-2148-9-259

32. Herrera JP, Dávalos LM. Phylogeny and divergence times of lemurs inferred with recent and ancient fossils in the tree. Syst Biol. 2016;65: 772–791. doi:10.1093/sysbio/syw035

33. Kistler L, Ratan A, Godfrey LR, Crowley BE, Hughes CE, Lei R, et al. Comparative and population mitogenomic analyses of Madagascar's extinct, giant 'subfossil' lemurs. J Hum Evol. 2015;79: 45–54. doi:10.1016/j.jhevol.2014.06.016

34. Tung J, Barreiro LB. The contribution of admixture to primate evolution. Curr Opin Genet Dev. 2017;47: 61–68. doi:10.1016/j.gde.2017.08.010

35. Stevens NJ, Seiffert ER, O'Connor PM, Roberts EM, Schmitz MD, Krause C, et al. Palaeontological evidence for an Oligocene divergence between Old World monkeys and apes. Nature. 2013;497: 611–614. doi:10.1038/nature12161

776 36. Huson DH, Klöpper T, Lockhart PJ, Steel MA. Reconstruction of reticulate
777 networks from gene trees. Proceedings of RECOMB 2005: The 9th Annual
778 International Conference Research in Computational Molecular Biology. Berlin:
779 Springer; 2005. pp. 233–249. doi:10.1007/11415770_18

780 37. Waterhouse RM, Seppey M, Simão FA, Manni M, Ioannidis P, Klioutchnikov G, et
781 al. BUSCO applications from quality assessments to gene prediction and
782 phylogenomics. Mol Biol Evol. 2018;35: 543–548. doi:10.1093/molbev/msx319

783 38. Zhang C, Rabiee M, Sayyari E, Mirarab S. ASTRAL-III: polynomial time species
784 tree reconstruction from partially resolved gene trees. BMC Bioinformatics.
785 2018;19: 153. doi:10.1186/s12859-018-2129-y

786 39. Minh BQ, Schmidt HA, Chernomor O, Schrempf D, Woodhams MD, von Haeseler
787 A, et al. IQ-TREE 2: new models and efficient methods for phylogenetic inference
788 in the genomic era. Mol Biol Evol. 2020 [cited 30 Mar 2020].
789 doi:10.1093/molbev/msaa015

790 40. Sayyari E, Mirarab S. Fast coalescent-based computation of local branch support
791 from quartet frequencies. Mol Biol Evol. 2016;33: 1654–1668.
792 doi:10.1093/molbev/msw079

793 41. Adkins RM, Honeycutt RL. Molecular phylogeny of the superorder Archonta. Proc
794 Natl Acad Sci. 1991;88: 10317–10321. doi:10.1073/pnas.88.22.10317

795 42. Arnason U, Adegoke JA, Bodin K, Born EW, Esa YB, Gullberg A, et al.
796 Mammalian mitogenomic relationships and the root of the eutherian tree. Proc
797 Natl Acad Sci. 2002;99: 8151–8156. doi:10.1073/pnas.102164299

798 43. Bloch JI, Boyer DM. Grasping primate origins. Science. 2002;298: 1606–1610.
799 doi:10.1126/science.1078249

800 44. Madsen O, Scally M, Douady CJ, Kao DJ, DeBry RW, Adkins R, et al. Parallel
801 adaptive radiations in two major clades of placental mammals. Nature. 2001;409:
802 610–614. doi:10.1038/35054544

803 45. Meredith RW, Janecka JE, Gatesy J, Ryder OA, Fisher CA, Teeling EC, et al.
804 Impacts of the Cretaceous terrestrial revolution and KPg extinction on mammal
805 diversification. Science. 2011;334: 521–524. doi:10.1126/science.1211028

806 46. Murphy WJ, Eizirik E, Johnson WE, Zhang YP, Ryder OA, O'Brien SJ. Molecular
807 phylogenetics and the origins of placental mammals. Nature. 2001;409: 614–618.
808 doi:10.1038/35054550

809 47. Murphy WJ, Eizirik E, O'Brien SJ, Madsen O, Scally M, Douady CJ, et al.
810 Resolution of the early placental mammal radiation using Bayesian phylogenetics.
811 Science. 2001;294: 2348–2351. doi:10.1126/science.1067179

812 48. Novacek MJ. Mammalian phylogeny: shaking the tree. Nature. 1992;356: 121–
813 125. doi:10.1038/356121a0

814 49. O'Leary MA, Bloch JI, Flynn JJ, Gaudin TJ, Giallombardo A, Giannini NP, et al.
815 The placental mammal ancestor and the post-K-Pg radiation of placentals.
816 Science. 2013;339: 662–667. doi:10.1126/science.1229237

817 50. Poux C, Douzery EJP. Primate phylogeny, evolutionary rate variations, and
818 divergence times: a contribution from the nuclear gene *IRBP*. Am J Phys
819 Anthropol. 2004;124: 1–16. doi:10.1002/ajpa.10322

820 51. Janečka JE, Miller W, Pringle TH, Wiens F, Zitzmann A, Helgen KM, et al.
821 Molecular and genomic data identify the closest living relative of primates.
822 Science. 2007;318: 792–794. doi:10.1126/science.1147555

823 52. Mason VC, Li G, Minx P, Schmitz J, Churakov G, Doronina L, et al. Genomic
824 analysis reveals hidden biodiversity within colugos, the sister group to primates.
825 Sci Adv. 2016;2: e1600633. doi:10.1126/sciadv.1600633

826 53. Schmitz J, Ohme M, Suryobroto B, Zischler H. The colugo (*Cynocephalus*
827 *variegatus*, Dermoptera): the primates' gliding sister? Mol Biol Evol. 2002;19:
828 2308–2312. doi:10.1093/oxfordjournals.molbev.a004054

829 54. Jarvis ED, Mirarab S, Aberer AJ, Li B, Houde P, Li C, et al. Whole-genome
830 analyses resolve early branches in the tree of life of modern birds. Science.
831 2014;346: 1320–1331. doi:10.1126/science.1253451

832 55. Pease JB, Haak DC, Hahn MW, Moyle LC. Phylogenomics reveals three sources
833 of adaptive variation during a rapid radiation. PLOS Biol. 2016;14: e1002379.
834 doi:10.1371/journal.pbio.1002379

835 56. Salichos L, Rokas A. Inferring ancient divergences requires genes with strong
836 phylogenetic signals. Nature. 2013;497: 327–331. doi:10.1038/nature12130

837 57. Minh BQ, Hahn MW, Lanfear R. New methods to calculate concordance factors
838 for phylogenomic datasets. bioRxiv. 2018; 487801. doi:10.1101/487801

839 58. Jameson NM, Hou Z-C, Sterner KN, Weckle A, Goodman M, Steiper ME, et al.
840 Genomic data reject the hypothesis of a prosimian primate clade. J Hum Evol.
841 2011;61: 295–305. doi:10.1016/j.jhevol.2011.04.004

842 59. Zachos J, Pagani M, Sloan L, Thomas E, Billups K. Trends, rhythms, and
843 aberrations in global climate 65 ma to present. Science. 2001;292: 686–693.
844 doi:10.1126/science.1059412

845 60. Yoder AD. The phylogenetic position of genus *Tarsius*: whose side are you on? In:
846 Wright PC, Simons EL, Gursky S, editors. Tarsiers past, present, and future.
847 Rutgers University Press; 2003.

61. Gregory WK. On the classification and phylogeny of the Lemuroidea. Bull Geol Soc Am. 1915; 426–446.

62. Pocock RI. On the external characters of the lemurs and of *Tarsius*. Proc Zool Soc Lond. 1918;88: 19–53. doi:10.1111/j.1096-3642.1918.tb02076.x

63. Hartig G, Churakov G, Warren WC, Brosius J, Makalowski W, Schmitz J. Retrophylogenomics place tarsiers on the evolutionary branch of anthropoids. Sci Rep. 2013;3: 1756. doi:10.1038/srep01756

64. Hayasaka K, Gojobori T, Horai S. Molecular phylogeny and evolution of primate mitochondrial DNA. Mol Biol Evol. 1988;5: 626–644. doi:10.1093/oxfordjournals.molbev.a040524

65. Jaworski CJ. A reassessment of mammalian αA-crystallin sequences using DNA sequencing: implications for anthropoid affinities of tarsier. J Mol Evol. 1995;41: 901–908. doi:10.1007/bf00173170

66. Whitfield JB, Lockhart PJ. Deciphering ancient rapid radiations. Trends Ecol Evol. 2007;22: 258–265. doi:10.1016/j.tree.2007.01.012

67. Bond M, Tejedor MF, Campbell KE, Chornogubsky L, Novo N, Goin F. Eocene primates of South America and the African origins of New World monkeys. Nature. 2015;520: 538–541. doi:10.1038/nature14120

68. Kubatko LS, Degnan JH. Inconsistency of phylogenetic estimates from concatenated data under coalescence. Syst Biol. 2007;56: 17–24. doi:10.1080/10635150601146041

69. Roch S, Steel M. Likelihood-based tree reconstruction on a concatenation of aligned sequence data sets can be statistically inconsistent. Theor Popul Biol. 2015;100: 56–62. doi:10.1016/j.tpb.2014.12.005

70. Warnow T. Concatenation analyses in the presence of incomplete lineage sorting. PLOS Curr Tree Life. 2015;7. doi:10.1371/currents.tol.8d41ac0f13d1abedf4c4a59f5d17b1f7

71. Bryant D, Hahn MW. The concatenation question. In: Scornavacca C, Delsuc F, Galtier N, editors. Phylogenetics in the Genomic Era. No commercial publisher | Authors open access book; 2020. pp. 3.4:1–3.4:23. Available: https://hal.archives-ouvertes.fr/hal-02535651

72. Sayyari E, Mirarab S. Testing for polytomies in phylogenetic species trees using quartet frequencies. Genes. 2018;9: 132. doi:10.3390/genes9030132

73. Liu L, Edwards SV. Phylogenetic analysis in the anomaly zone. Syst Biol. 2009;58: 452–460. doi:10.1093/sysbio/syp034

883 74. Swofford DL. PAUP*. Phylogenetic Analysis Using Parsimony (*and other
884 methods). Sinauer Assoc Sunderland Mass. 2002;Version 4.

885 75. Mendes FK, Livera AP, Hahn MW. The perils of intralocus recombination for
886 inferences of molecular convergence. Philos Trans R Soc Lond B Biol Sci.
887 2019;374: 20180244. doi:10.1098/rstb.2018.0244

888 76. Springer MS, Gatesy J. The gene tree delusion. Mol Phylogenet Evol. 2016;94: 1–
889 33. doi:10.1016/j.ympev.2015.07.018

890 77. Hoang DT, Vinh LS, Flouri T, Stamatakis A, von Haeseler A, Minh BQ. MPBoot:
891 fast phylogenetic maximum parsimony tree inference and bootstrap
892 approximation. BMC Evol Biol. 2018;18: 11–11. doi:10.1186/s12862-018-1131-3

893 78. Mendes FK, Hahn MW. Gene tree discordance causes apparent substitution rate
894 variation. Syst Biol. 2016;65: 711–721. doi:10.1093/sysbio/syw018

895 79. Brunet M, Guy F, Pilbeam D, Mackaye HT, Likius A, Ahounta D, et al. A new
896 hominid from the Upper Miocene of Chad, Central Africa. Nature. 2002;418: 145–
897 151. doi:10.1038/nature00879

898 80. Sigé B, Jaeger J-J, Sudre J, Vianey-Liaud M. Altiatlasius koulchii n. gen. et sp.,
899 primate omomyidé du Paléocène supérieur du Maroc, et les origines des
900 euprimates. Palaeontogr Abt A. 1990; 31–56.

901 81. Lartillot N, Lepage T, Blanquart S. PhyloBayes 3: a Bayesian software package
902 for phylogenetic reconstruction and molecular dating. Bioinformatics. 2009;25:
903 2286–2288. doi:10.1093/bioinformatics/btp368

904 82. Goodman M, Porter CA, Czelusniak J, Page SL, Schneider H, Shoshani J, et al.
905 Toward a phylogenetic classification of Primates based on DNA evidence
906 complemented by fossil evidence. Mol Phylogenet Evol. 1998;9: 585–598.
907 doi:10.1006/mpev.1998.0495

908 83. Wilkinson RD, Steiper ME, Soligo C, Martin RD, Yang Z, Tavaré S. Dating primate
909 divergences through an integrated analysis of palaeontological and molecular
910 data. Syst Biol. 2011;60: 16–31. doi:10.1093/sysbio/syq054

911 84. Yoder AD, Yang Z. Divergence dates for Malagasy lemurs estimated from multiple
912 gene loci: geological and evolutionary context. Mol Ecol. 2004;13: 757–773.
913 doi:10.1046/j.1365-294X.2004.02106.x

914 85. Benton MJ, Donoghue PCJ, Asher RJ, Friedman M, Near TJ, Vinther J.
915 Constraints on the timescale of animal evolutionary history. Palaeontol Electron.
916 2015;18.1.1FC: 1–106. doi:10.26879/424

86. Edwards SV, Beerli P. Perspective: gene divergence, population divergence, and the variance in coalescence time in phylogeographic studies. Evolution. 2000;54: 1839–1854. doi:10.1111/j.0014-3820.2000.tb01231.x

87. Rogers J. Levels of the genealogical hierarchy and the problem of hominoid phylogeny. Am J Phys Anthropol. 1994;94: 81–88. doi:10.1002/ajpa.1330940107

88. Carbone L, Harris RA, Gnerre S, Veeramah KR, Lorente-Galdos B, Huddleston J, et al. Gibbon genome and the fast karyotype evolution of small apes. Nature. 2014;513: 195–201. doi:10.1038/nature13679

89. Veeramah KR, Woerner AE, Johnstone L, Gut I, Gut M, Marques-Bonet T, et al. Examining phylogenetic relationships among gibbon genera using whole genome sequence data using an approximate bayesian computation approach. Genetics. 2015;200: 295–308. doi:10.1534/genetics.115.174425

90. Fan Z, Zhao G, Li P, Osada N, Xing J, Yi Y, et al. Whole-genome sequencing of tibetan macaque (*Macaca thibetana*) provides new insight into the macaque evolutionary history. Mol Biol Evol. 2014;31: 1475–1489. doi:10.1093/molbev/msu104

91. Yan G, Zhang G, Fang X, Zhang Y, Li C, Ling F, et al. Genome sequencing and comparison of two nonhuman primate animal models, the cynomolgus and Chinese rhesus macaques. Nat Biotechnol. 2011;29: 1019–1023. doi:10.1038/nbt.1992

92. Hahn MW. Molecular population genetics. First Edition. Oxford, New York: Oxford University Press; 2018.

93. Patterson N, Moorjani P, Luo Y, Mallick S, Rohland N, Zhan Y, et al. Ancient admixture in human history. Genetics. 2012;192: 1065–1093. doi:10.1534/genetics.112.145037

94. Osada N, Uno Y, Mineta K, Kameoka Y, Takahashi I, Terao K. Ancient genome-wide admixture extends beyond the current hybrid zone between *Macaca fascicularis* and *M. mulatta*. Mol Ecol. 2010;19: 2884–2895. doi:10.1111/j.1365-294X.2010.04687.x

94. Koufos GD. Potential hominoid ancestors for Hominidae. Henke W, Tattersall I, editors. Handbook of Paleoanthropology. Berlin: Springer; 2007. pp. 1761–1790. doi:10.1007/978-3-642-39979-4_44

96. Patterson N, Richter DJ, Gnerre S, Lander ES, Reich D. Genetic evidence for complex speciation of humans and chimpanzees. Nature. 2006;441: 1103–1108. doi:10.1038/nature04789

952 97. Than C, Ruths D, Nakhleh L. PhyloNet: a software package for analyzing and
953 reconstructing reticulate evolutionary relationships. BMC Bioinformatics. 2008;9:
954 322. doi:10.1186/1471-2105-9-322

955 97. Wen D, Yu Y, Zhu J, Nakhleh L. Inferring phylogenetic networks using Phylonet.
956 Syst Biol. 2018;67: 735–740. doi:10.1093/sysbio/syy015

957 99. Roos C, Kothe M, Alba DM, Delson E, Zinner D. The radiation of macaques out of
958 Africa: Evidence from mitogenome divergence times and the fossil record. J Hum
959 Evol. 2019;133: 114–132. doi:10.1016/j.jhevol.2019.05.017

960 100. Belmaker M. The presence of a large cercopithecine (cf. Theropithecus sp.) in the
961 'Ubeidiya formation (Early Pleistocene, Israel). J Hum Evol. 2010;58: 79–89.
962 doi:10.1016/j.jhevol.2009.08.004

963 101. Hughes JK, Elton S, O'Regan HJ. Theropithecus and "Out of Africa" dispersal in
964 the Plio-Pleistocene. J Hum Evol. 2008;54: 43–77.
965 doi:10.1016/j.jhevol.2007.06.004

966 102. Larrasoaña JC, Roberts AP, Rohling EJ, Winklhofer M, Wehausen R. Three
967 million years of monsoon variability over the northern Sahara. Clim Dyn. 2003;21:
968 689–698. doi:10.1007/s00382-003-0355-z

969 103. Larrasoaña JC, Roberts AP, Rohling EJ. Dynamics of green Sahara periods and
970 their role in hominin evolution. PLOS One. 2013;8: e76514.
971 doi:10.1371/journal.pone.0076514

972 104. Vaks A, Woodhead J, Bar-Matthews M, Ayalon A, Cliff RA, Zilberman T, et al.
973 Pliocene–Pleistocene climate of the northern margin of Saharan–Arabian Desert
974 recorded in speleothems from the Negev Desert, Israel. Earth Planet Sci Lett.
975 2013;368: 88–100. doi:10.1016/j.epsl.2013.02.027

976 105. Coulthard TJ, Ramirez JA, Barton N, Rogerson M, Brücher T. Were rivers flowing
977 across the Sahara during the last interglacial? Implications for human migration
978 through Africa. PloS One. 2013;8: e74834. doi:10.1371/journal.pone.0074834

979 106. Sahnouni M, Parés JM, Duval M, Cáceres I, Harichane Z, van der Made J, et al.
980 1.9-million- and 2.4-million-year-old artifacts and stone tool-cutmarked bones from
981 Ain Boucherit, Algeria. Science. 2018;362: 1297–1301.
982 doi:10.1126/science.aau0008

983 107. deMenocal PB. African climate change and faunal evolution during the Pliocene–
984 Pleistocene. Earth Planet Sci Lett. 2004;220: 3–24. doi:10.1016/S0012-
985 821X(04)00003-2

986 108. Slatkin M, Pollack JL. Subdivision in an ancestral species creates asymmetry in
987 gene trees. Mol Biol Evol. 2008;25: 2241–2246. doi:10.1093/molbev/msn172

988 109. Gernhard T. New analytic results for speciation times in neutral models. Bull Math
989 Biol. 2008;70: 1082–1097. doi:10.1007/s11538-007-9291-0

990 110. Gligor M, Ganzhorn JU, Rakotondravony D, Ramilijaona OR, Razafimahatratra E,
991 Zischler H, et al. Hybridization between mouse lemurs in an ecological transition
992 zone in southern Madagascar. Mol Ecol. 2009;18: 520–533. doi:10.1111/j.1365-
993 294X.2008.04040.x

994 111. Pastorini J, Zaramody A, Curtis DJ, Nievergelt CM, Mundy NI. Genetic analysis of
995 hybridization and introgression between wild mongoose and brown lemurs. BMC
996 Evol Biol. 2009;9: 32. doi:10.1186/1471-2148-9-32

997 112. Williams RC, Blanco MB, Poelstra JW, Hunnicutt KE, Comeault AA, Yoder AD.
998 Conservation genomic analysis reveals ancient introgression and declining levels
999 of genetic diversity in Madagascar's hibernating dwarf lemurs. Heredity. 2020;124:
1000 236–251. doi:10.1038/s41437-019-0260-9

1001 113. Wyner YM, Johnson SE, Stumpf RM, Desalle R. Genetic assessment of a white-
1002 collared×red-fronted lemur hybrid zone at Andringitra, Madagascar. Am J
1003 Primatol. 2002;57: 51–66. doi:10.1002/ajp.10033

1004 114. Gnerre S, MacCallum I, Przybylski D, Ribeiro FJ, Burton JN, Walker BJ, et al.
1005 High-quality draft assemblies of mammalian genomes from massively parallel
1006 sequence data. Proc Natl Acad Sci. 2011;108: 1513–1518.
1007 doi:10.1073/pnas.1017351108

1008 114. English AC, Richards S, Han Y, Wang M, Vee V, Qu J, et al. Mind the gap:
1009 upgrading genomes with Pacific Biosciences RS long-read sequencing
1010 technology. PLOS ONE. 2012;7: e47768. doi:10.1371/journal.pone.0047768

1011 116. Altschul SF, Gish W, Miller W, Myers EW, Lipman DJ. Basic local alignment
1012 search tool. J Mol Biol. 1990;215: 403–410. doi:10.1016/S0022-2836(05)80360-2

1013 117. Camacho C, Coulouris G, Avagyan V, Ma N, Papadopoulos J, Bealer K, et al.
1014 BLAST+: architecture and applications. BMC Bioinformatics. 2009;10: 421.
1015 doi:10.1186/1471-2105-10-421

1016 118. van Dongen S. Graph clustering by flow simulation. PhD thesis, University of
1017 Utrecht. 2000. Available:
1018 http://www.library.uu.nl/digiarchief/dip/diss/1895620/full.pdf

1019 119. Wattam AR, Abraham D, Dalay O, Disz TL, Driscoll T, Gabbard JL, et al. PATRIC,
1020 the bacterial bioinformatics database and analysis resource. Nucleic Acids Res.
1021 2014;42: D581–D591. doi:10.1093/nar/gkt1099

1022 120. Sela I, Ashkenazy H, Katoh K, Pupko T. GUIDANCE2: accurate detection of
1023 unreliable alignment regions accounting for the uncertainty of multiple parameters.
1024 Nucleic Acids Res. 2015;43: W7–14. doi:10.1093/nar/gkv318

121. Katoh K, Standley DM. Mafft multiple sequence alignment software version 7: improvements in performance and usability. Mol Biol Evol. 2013;30: 772–780. doi:10.1093/molbev/mst010

122. Capella-Gutiérrez S, Silla-Martínez JM, Gabaldon T. trimAl: a tool for automated alignment trimming in large-scale phylogenetic analyses. Bioinformatics. 2009;25: 1972–1973. doi:10.1093/bioinformatics/btp348

123. Chernomor O, von Haeseler A, Minh BQ. Terrace aware data structure for phylogenomic inference from supermatrices. Syst Biol. 2016;65: 997–1008. doi:10.1093/sysbio/syw037

123. Hoang DT, Chernomor O, von Haeseler A, Minh BQ, Vinh LS. UFBoot2: improving the ultrafast bootstrap approximation. Mol Biol Evol. 2018;35: 518–522. doi:10.1093/molbev/msx281

125. Kalyaanamoorthy S, Minh BQ, Wong TKF, von Haeseler A, Jermiin LS. ModelFinder: fast model selection for accurate phylogenetic estimates. Nat Methods. 2017;14: 587–589. doi:10.1038/nmeth.4285

126. Eaton DAR, Ree RH. Inferring phylogeny and introgression using RADseq data: an example from flowering plants (*Pedicularis*: Orobanchaceae). Syst Biol. 2013;62: 689–706. doi:10.1093/sysbio/syt032

127. Dunn OJ. Confidence intervals for the means of dependent, normally distributed variables. J Am Stat Assoc. 1959;54: 613–621. doi:10.2307/2282541

128. Sidak Z. Rectangular confidence regions for the means of multivariate normal distributions. J Am Stat Assoc. 1967;62: 626–633. doi:10.2307/2283989

129. Lartillot N, Philippe H. A Bayesian mixture model for across-site heterogeneities in the amino-acid replacement process. Mol Biol Evol. 2004;21: 1095–1109. doi:10.1093/molbev/msh112

130. Thorne JL, Kishino H, Painter IS. Estimating the rate of evolution of the rate of molecular evolution. Mol Biol Evol. 1998;15: 1647–1657.

131. Fleagle JG. Apes and humans. Primate adaptation and evolution. Elsevier; 2013. pp. 151–168. doi:10.1016/B978-0-12-378632-6.00007-0

Supplementary Information

Table S1. Genomes analyzed in this study with the original NCBI release date, the publication for the reference used, and the accession number for the assembly. When possible the most recent version for each genome was used.

Table S2. All published genomes used in this study, including links to the assemblies and NCBI BioProjects. Annotation information is included for each genome at the time of download.

Table S3. Gaps/Ambiguities by species, and as a percentage of total alignment length. * denotes species sequenced this study.

Table S4. Lengths for each 40-locus concatenated alignment used in the molecular dating analyses. Each dataset was analyzed twice until node age estimates converged (15-25k steps) using a log-normal auto-correlated model (Thorne et al. 1998).

Table S5. Fossil calibrations employed in this study. Node numbering corresponds to the numbering in Figure 3. Median underflow/overflow for each calibration was calculated from 20 independent runs performed on 10 datasets (2 runs per dataset).

Table S6. Mean node age for 20 independent Phylobayes dating runs. Node numbers correspond to the numbering in Figure 3. The 95% HPD intervals were calculated by averaging the minimum and maximum of the 95% HPD interval for each dating run.

Table S7. Quartets used to test for significant Δ values for internal branches of the primate tree. Branches tested correspond to the labeled branches in Figure 3. After correcting for multiple comparisons (Dunn-Šidák, $P = 0.00301$), three internal branches and 8 quartets were found to have significant Δ values, indicating a likely introgression event.

Supplementary Figure S1. Present day species distributions for four African Papionini (*Papio, Theropithecus, Mandrillus*, and *Cercocebus*) and three Asian *Macaca* species included in the introgression analysis. The ancestral *Macaca* distribution (grey shading) is inferred from *Macaca* fossil localities in Africa and Europe as reviewed in Roos et al. (2019). The ancestral *Macaca* distribution likely represents only a fraction of the species range from the late Miocene to the late Pleistocene in Africa and Europe. The contemporary distribution of the African *Macaca sylvanus* (bright green) is included for reference. Fossil localities for *Theropithecus* species hypothesized to overlap contemporaneously with various ancestral *Macaca* are included. Citations for spatial data of extant species: *Macaca nemistrina* (Richardson et al., 2008), *Macaca fascicularis* (Ong & Richardson, 2008), *Macaca sylvanus* (Butynski et al., 2008), *Macaca mulatta* (Timmins et al., 2008), *Theropithecus gelada* (Gippoliti et al., 2019), *Papio anubis* (Kingdon et al., 2008), *Cercocebus atys* (Oates et al., 2016), and *Mandrillus leucophaeus* (Oates & Butynski, 2008).

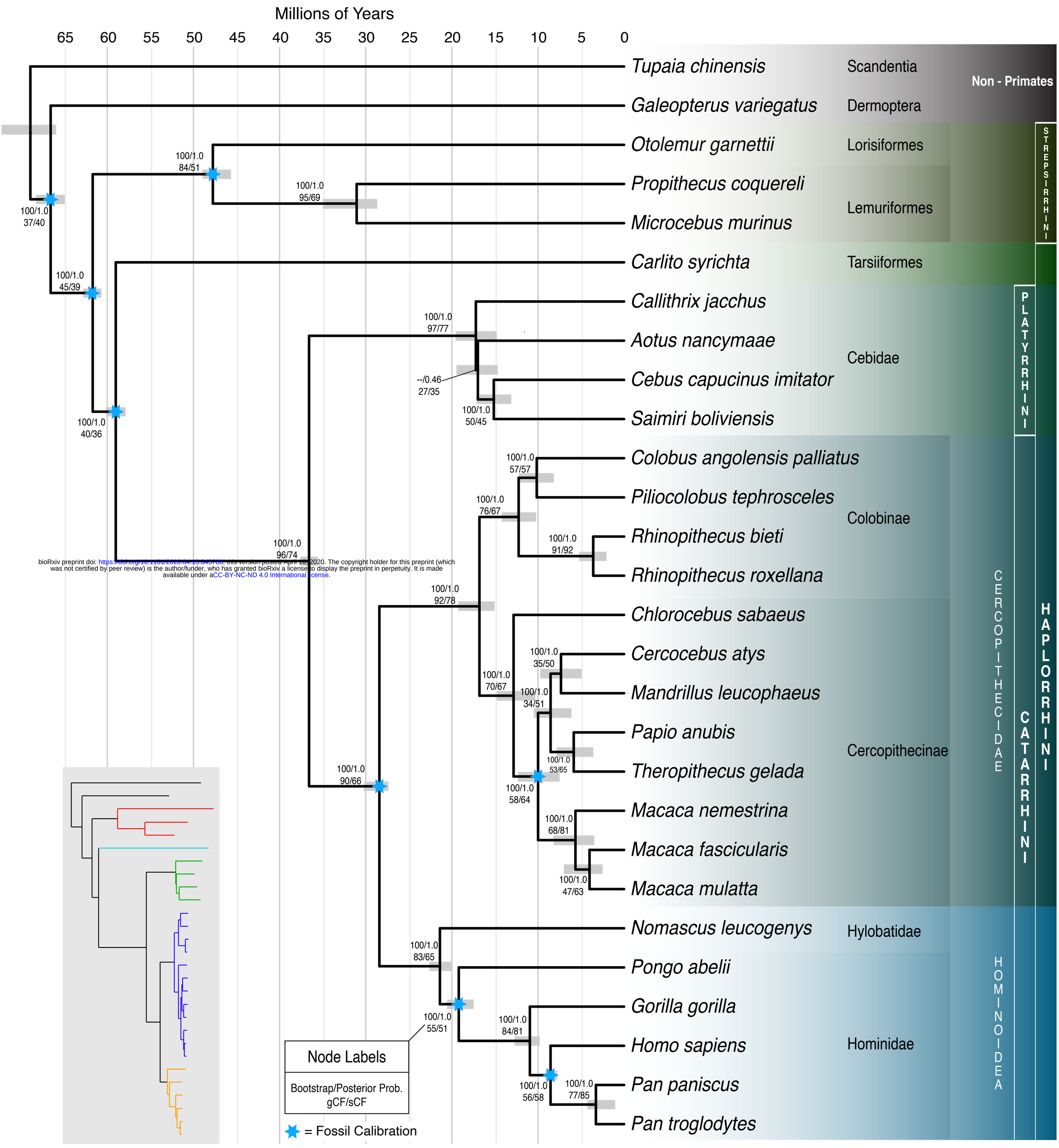

Figure 1.

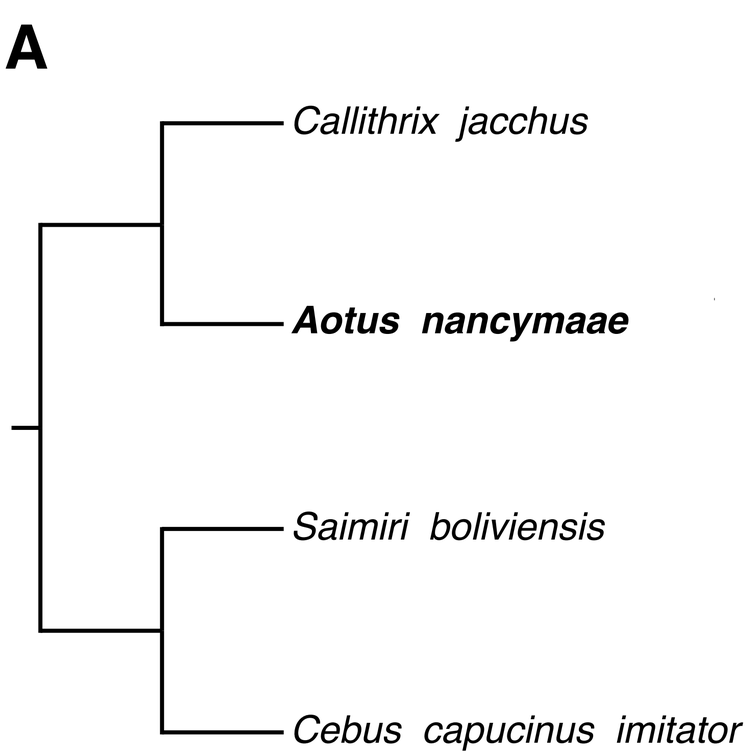

Tree 1
(ML-CONCAT)

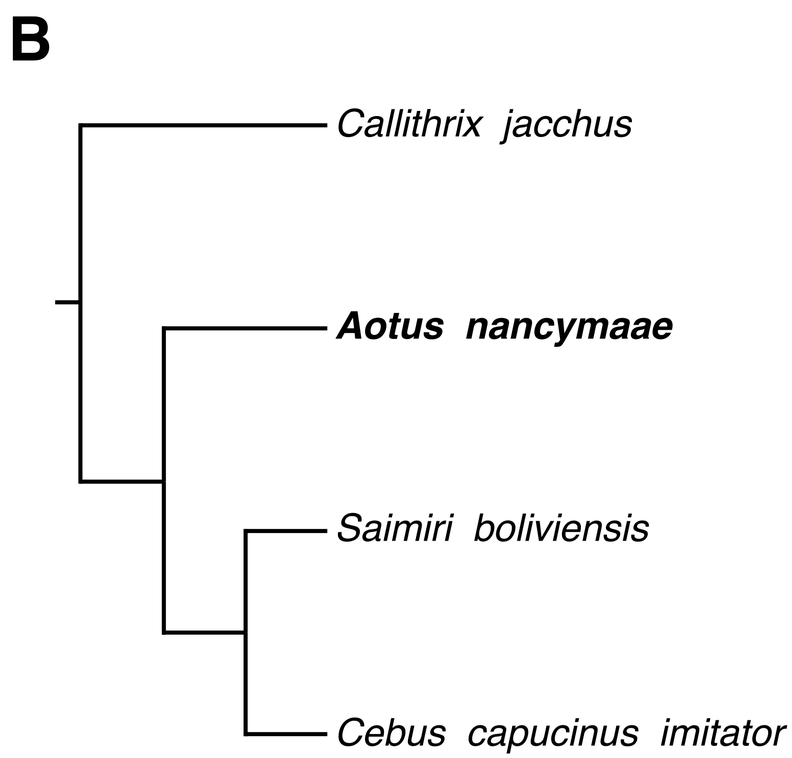

Tree 2
(ML-ASTRAL, MP-ASTRAL, MP-CONCAT)

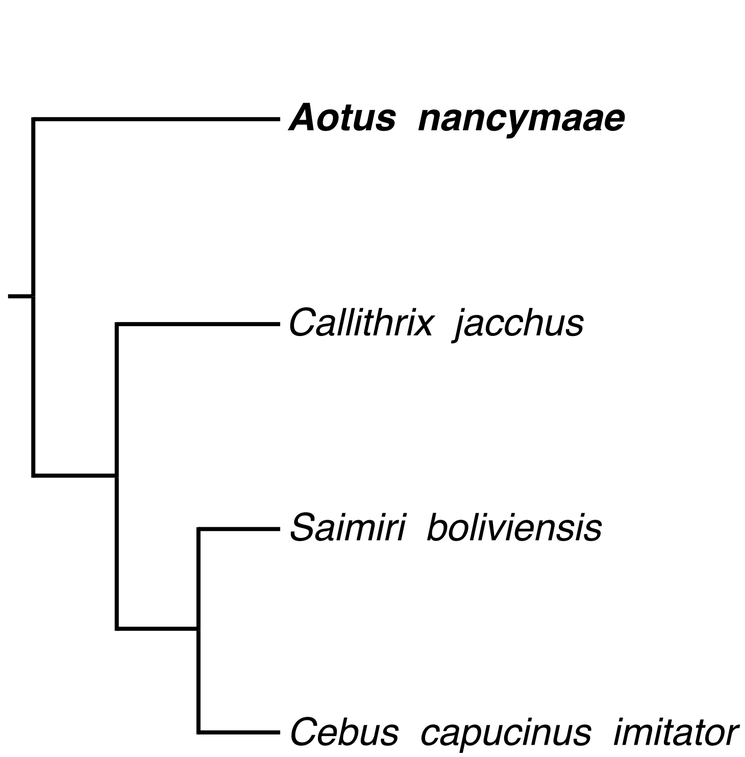

Tree 3

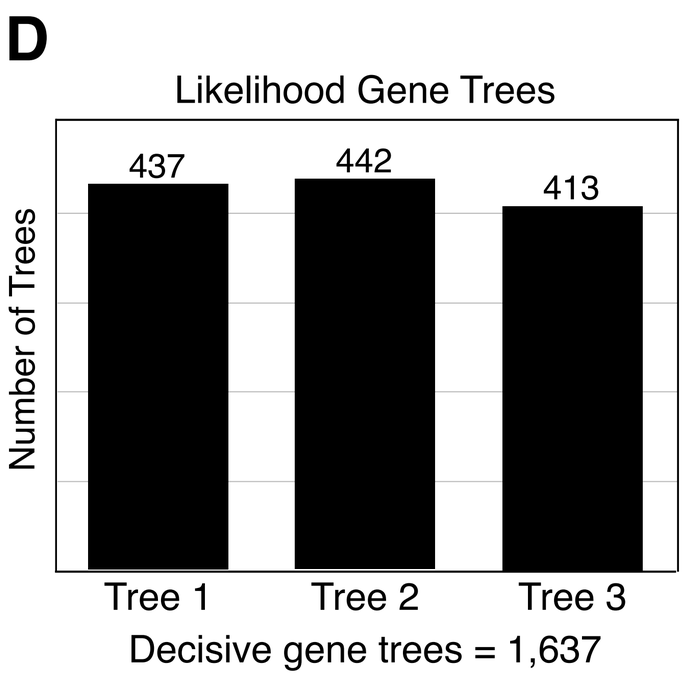

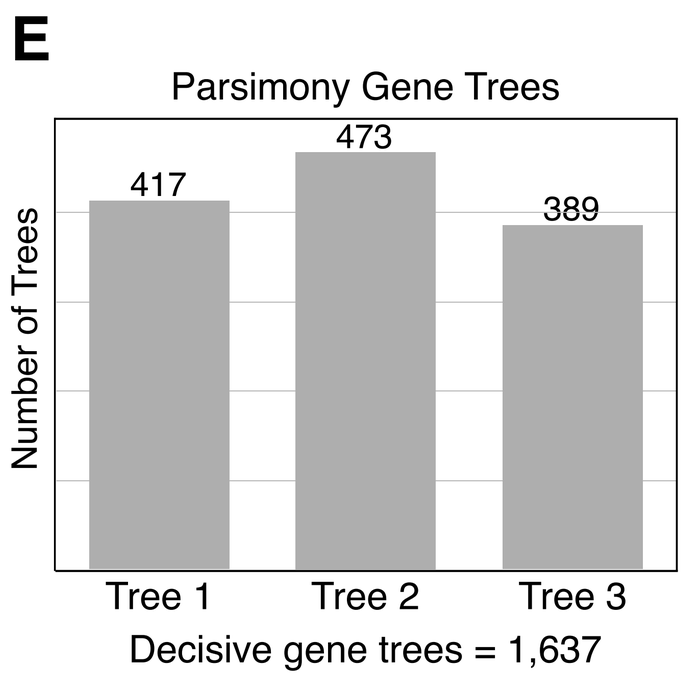

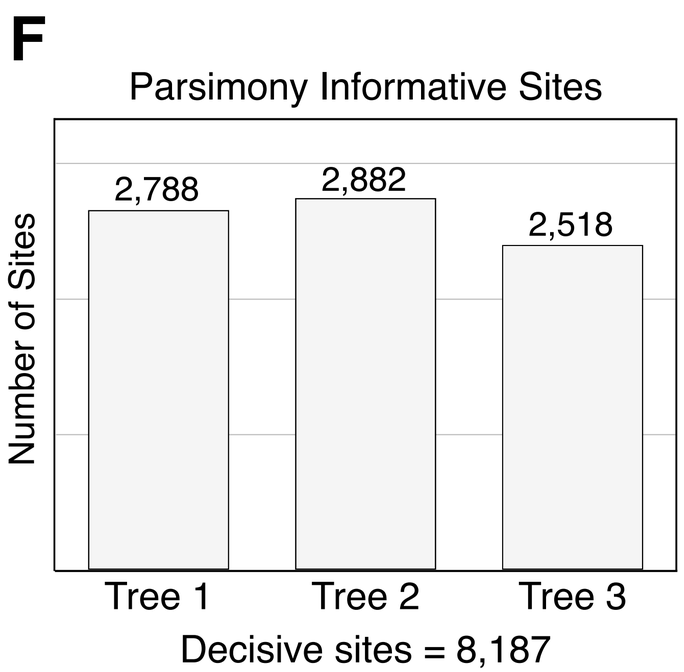

Figure 2.

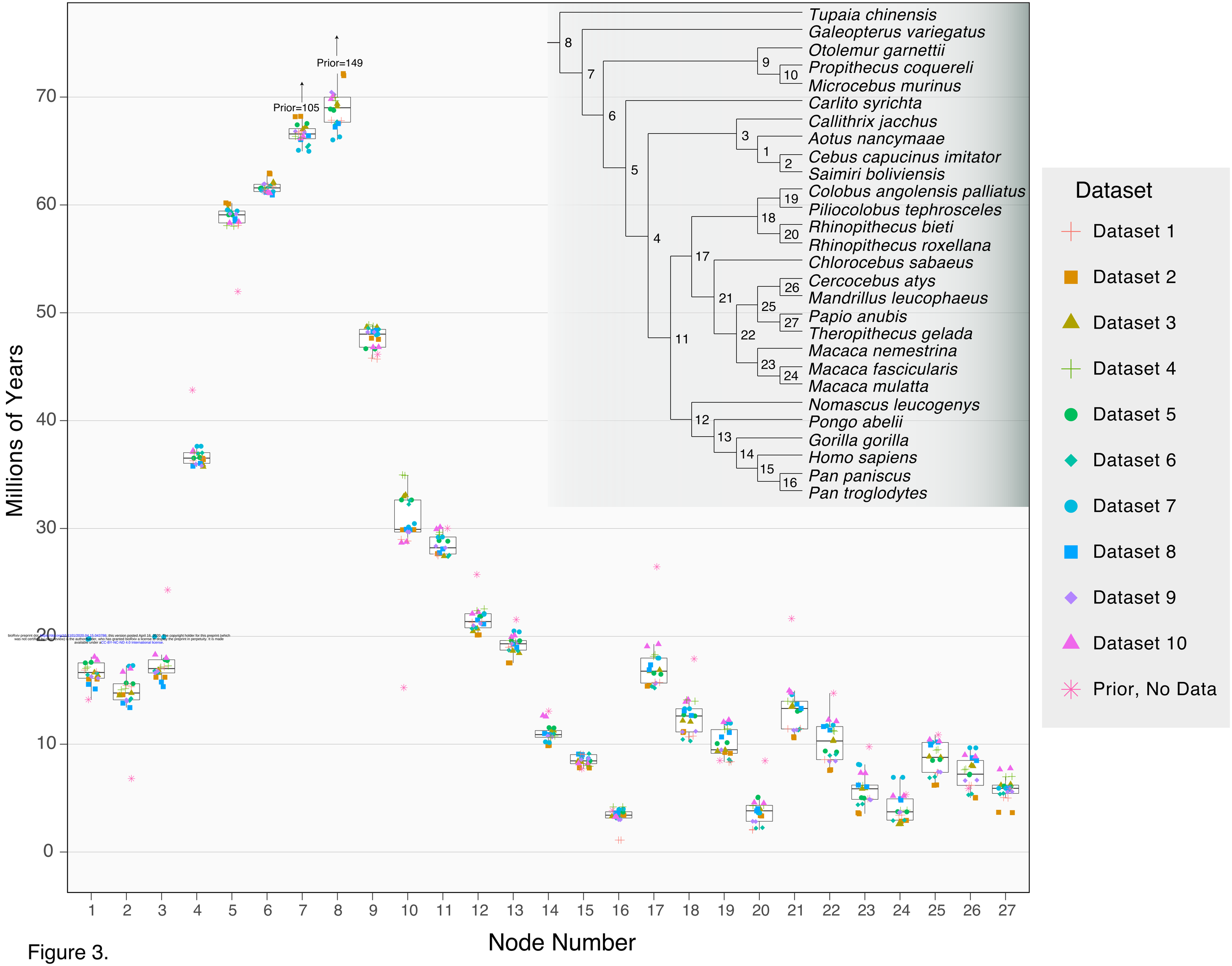

Figure 3.

Papionini

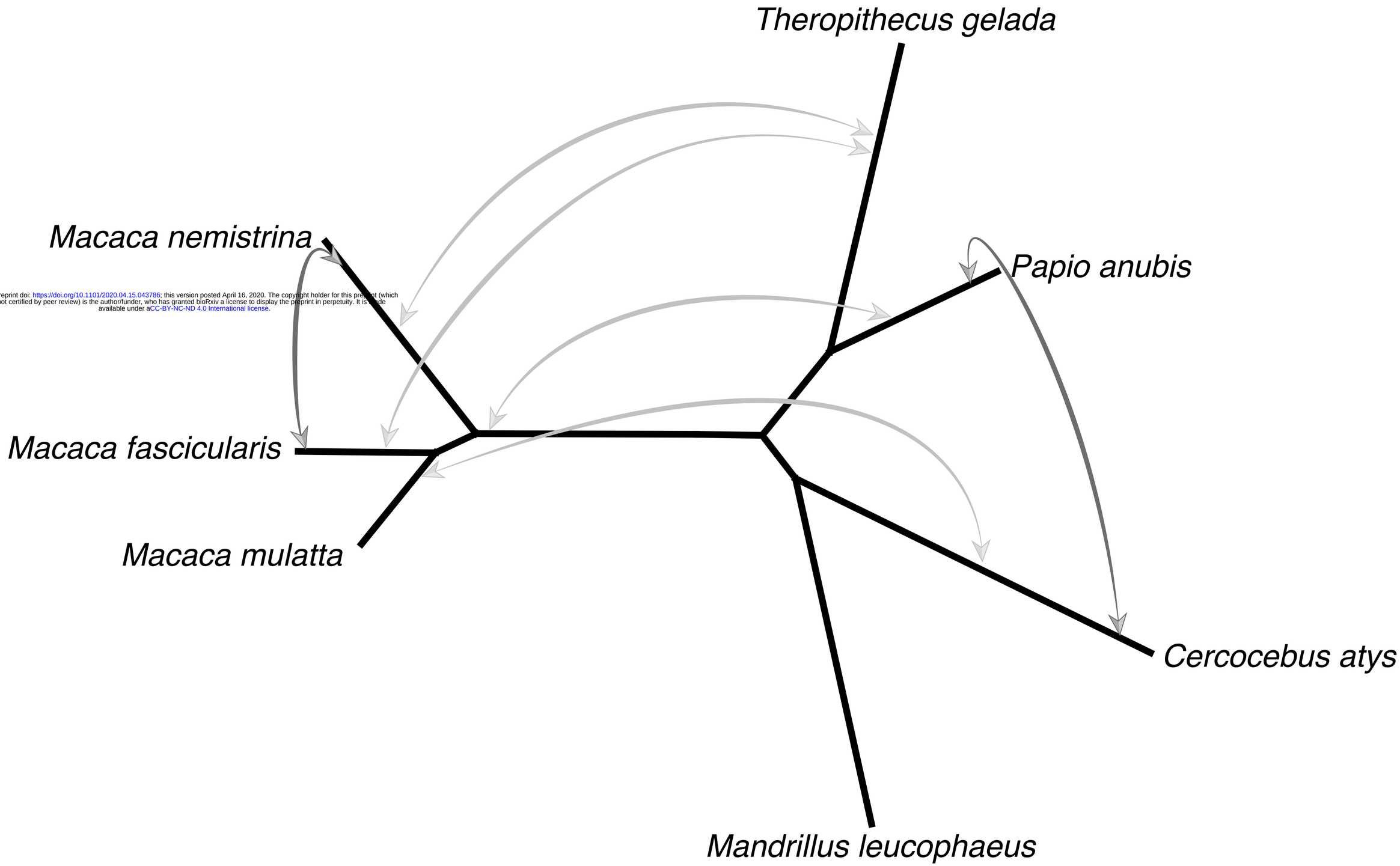

Figure 4.

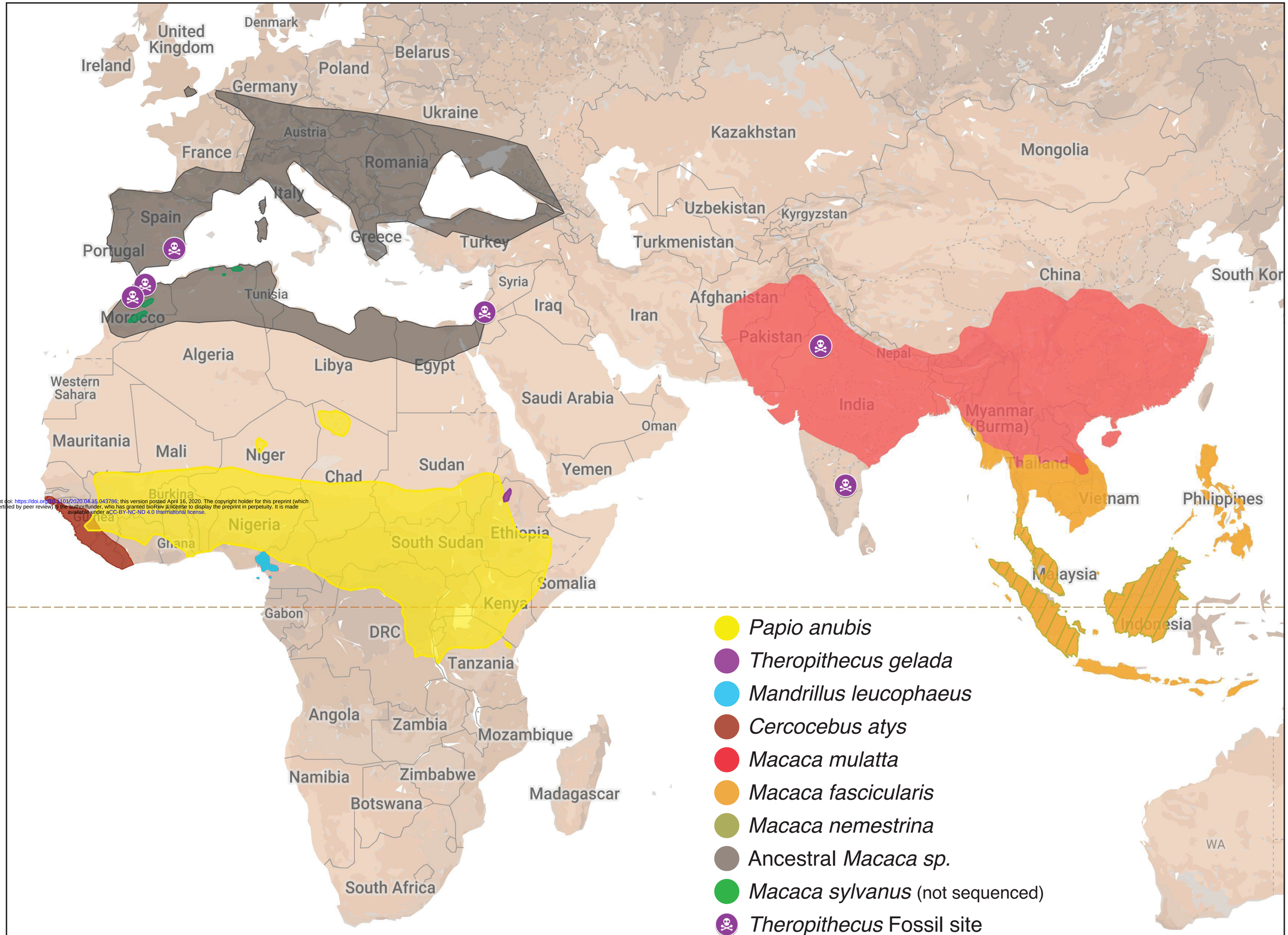

Supplementary Figure S1